Memoirs of the Faculty of Science, Kyoto University, Series of Physics, Astrophysics, Geophysics and Chemistry, Vol. XXXVIII, No. 2, Article 2, 1992

Focal Mechanisms of Earthquakes in the Hindukush-Pamir Region and its Tectonic Implication

By

Jiren XU[1], Zhixin, ZHAO[2] and Kazuo OIKE[1]

[1]Department of Geophysics, Faculty of Science, Kyoto University
[2]Institute of Geophysics, State Seismological Bureau, China

(Received December 20, 1991)

Abstract

Characteristics of focal mechanisms of shallow and intermediate depth earthquakes occurring in the Hindukush-Pamir region have been analyzed in detail based on mechanism solutions of 130 earthquakes. Their magnitude range (Mb) is from 4.7 to 6.3 and they distribute from the surface to 231 km deep. Data of source parameters and P wave initial motions were obtained from the Bulletin of the International Seismological Center during the period from 1971 to 1980.

The result indicates that there exists the subduction zone of the Indo-Australian plate relatively moving towards the Eurasian plate in the eastern Hindukush region. There is the distribution of stress field of down-dip extension within this subduction zone where P-axes are perpendicular to the slab and T-axes are parallel to the dip direction of the slab. The northward drift of the Hindukush subduction zone causes the compression with the N-S direction in the intermediate depth segment and the lateral ejection in the crust. It controls the crustal stress field in the Hindukush-Pamir region. The lateral ejection leads P-axes to turn to the NWN-SES direction in the western Hindukush, the Pamir and the South Tianshan regions which are located to the north and west of the subduction zone, and P-axes to turn to the NE-SW direction in the western Himalayan and Kashmir regions which are located to the east of the subduction zone. The tectonic force from the subduction makes a shallow block in the north of the Hindukush subduction zone upthrust along fault. The existence of the shallow seismic gap to the north of the subduction zone and the mechanism of many reverse faulting events in the Pamir region can be explained by such a structure.

1. Introduction

The Hindukush-Pamir region is located to the northwest of the Indian subcontinent near the northwestern boundary between the Indo-Australian and Eurasian plates. There is a junction of several famous mountain ranges, such as the Himalayan, Pamir, Hindukush, Karakorum and Tianshan mountains. Many active faults lie in this region (Fig. 1). It is one of the most seismic active regions in the world. The seismic activity along active faults is attributed to the collision of the northward-moving Indo-Australian plate to the Eurasian plate (Zhao et al., 1988). A lot of shallow earthquakes distribute in the Hindukush-Pamir region and its surroundings. Many intermediate depth earthquakes, however, concentrate only in a small area in the Hindukush-Pamir region. The deepest earthquakes occurred

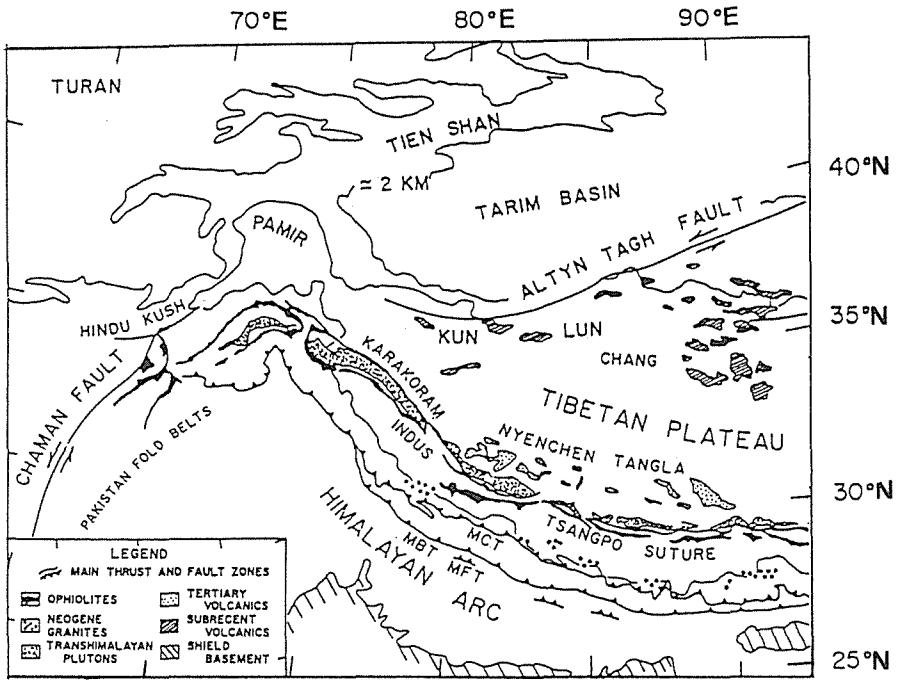

Fig. 1. Simplified map of active tectonics in the Hindukush-Pamir and the surrounding regions (from Ni, J. and M. Barazangi, 1984).

here in the depth about 260 km (Ning et al., 1990). The pattern of hypocentral distribution here is different from that in the Himalayan collision zone between the Indo-Australian and the Eurasian plates (Xu et al., 1988). Vertical profiles of hypocentral distributions of shallow and intermediate depth earthquakes in this region for the N-S and NW-SE directions show the V-shaped distribution (Santo et al., 1969). Such V-shaped distribution in this region differs from distributions in other regions where intermediate depth earthquakes occur.

Many significant results on geology, geodesy and seismicity in the Hindukush-Pamir region have been reported. The Indus Suture Zone has been found and investigated (Gausser., 1977). The velocity of the relative northward crustal motion of the Pamirs is 1.5 cm/yr which was observed by the measurement of local surface deformations between the Pamir and the Alai mountains (Kakkuri et al., 1986). These evidences provided us with materials to discuss the relative motion in the region between the Indo-Australian and Eurasian plates. The existence of a relative high Q value zone in the region from the north to the south of the Hindukush-Pamir intermediate depth earthquake zone (Khalturin et al., 1977) and of a high-velocity zone in and around the Hindukush-Pamir intermediate depth earthquake zone (Vinnik et al., 1977) suggests a variety of possible configurations of the subduction of oceanic or continental lithospheres. Chatelain et al. (1980) analyzed the activity of microearthquakes and fault plane solutions in the Hindukush region and inferred that the subduction of the oceanic lithosphere possibly took

place in this region. Roecker et al. (1980) pointed out that the distribution of earthquakes and the fault plane solutions in the Hindukush-Pamir region were grossly similar to those in other island arcs and that at the same time there was a variation in the fault plane solutions in this region much larger than that in the island arcs. However, Verma et al. (1985) has pointed out that the nature of focal mechanism solutions and dip of seismic zones in the Hindukush-Pamir region are too complex to be explained by a simple subduction model. Sugi et al. (1990) also analyzed 15 intermediate depth earthquakes which occurred in the Hindukush region and pointed out the complexity in the geological structure and the stress state there.

In this study, we determine 119 new focal mechanisms and investigate the regional characteristics of focal mechanisms of shallow and intermediate depth earthquakes in the Hindukush-Pamir region. The earthquake-generating stress field and its tectonic implication between the Indo-Australian and Eurasian plates are investigated on basis of the three dimensional distribution of earthquake mechanisms.

2. Data and method of analyses

Data used to get new solutions of mechanisms in this study were obtained from the Bulletin of the International Seismological Center. Source parameters and initial motions of 251 large and moderate earthquakes (Mb > 4.5) in this region from 1971 to 1980 whose initial motion data were reported at more than 8 stations were

Table 1. List of earthquake mechanism solutions used in this paper

Date	Origin Time	Lat. (°N)	Long. (°E)	Depth (km)	Mb	N-axes Az.	N-axes Pl.	P-axes Az.	P-axes Pl.	T-axes Az.	T-axes Pl.
Feb. 6, 1971	22:12	35°57.0'	69°47.0'	119	5.0	279	29	184	10	76	59
Mar. 23, 1971	9:52	41°26.0'	79°10.0'	29	5.7	33	27	300	6	199	62
Mar. 23, 1971	20:47	41°25.0'	79°12.0'	14	5.8	11	35	281	1	190	54
May. 9, 1971	19:26	35°32.0'	71° 4.0'	82	5.5	195	18	84	48	299	37
May. 10, 1971	14:51	42°51.0'	71°17.0'	14	5.6	44	42	136	2	229	48
Jun. 15, 1971	7:39	41°24.0'	79°23.0'	17	5.4	103	3	193	0	292	86
Jun. 15, 1971	22: 4	41°23.0'	79°11.0'	96	5.3	56	46	160	14	263	41
Aug. 4, 1971	0:24	36°25.0'	70°44.0'	207	5.6	303	21	207	17	80	63
Oct. 14, 1971	21:55	36°30.0'	71° 9.0'	82	5.0	185	59	303	16	41	26
Oct. 28, 1971	13:30	41°53.0'	72°21.0'	15	5.4	286	33	191	8	88	56
Nov. 18, 1971	7:31	38°26.0'	66°47.0'	28	5.2	244	28	334	1	66	62
Jan. 12, 1972	18:37	37°41.0'	75° 4.0'	96	5.3	185	76	40	12	309	8
Jan. 15, 1972	20:21	40°10.0'	78°58.0'	10	5.4	337	67	175	23	82	6
Jan. 20, 1972	11:36	36°23.0'	70°43.0'	214	5.8	179	35	85	5	348	54
Jan. 25, 1972	5:41	35°34.0'	69°50.0'	96	5.2	203	10	109	22	316	66
Feb. 22, 1972	1:14	36°28.0'	70°32.0'	213	5.2	100	38	215	28	330	40
May. 30, 1972	6:38	38°26.0'	69°31.0'	20	4.9	28	43	119	1	210	47
Jun. 20, 1972	5:26	36°34.0'	71°34.0'	99	5.1	84	6	177	23	340	66
Jun. 24, 1972	15:29	36°17.0'	69°41.0'	47	5.9	37	21	297	24	163	58
Jul. 8, 1972	6:49	36°26.0'	71°25.0'	105	5.6	68	5	337	8	188	81
Jul. 11, 1972	5:54	36°28.0'	70°43.0'	199	5.1	93	29	201	30	328	46
Sep. 3, 1972	16:48	35°56.0'	73°20.0'	45	6.2	194	23	97	17	334	61
Sep. 4, 1972	13:42	35°55.0'	73°21.0'	57	5.7	296	56	137	32	41	10
Sep. 17, 1972	17:37	35°56.0'	73°19.0'	49	5.4	33	4	125	29	296	61
Sep. 27, 1972	2: 3	33°59.0'	72°42.0'	41	5.1	305	59	136	31	43	5
Oct. 13, 1972	5: 4	35°54.0'	73°19.0'	60	5.2	28	62	199	28	291	4
Nov. 3, 1972	23:58	34° 7.0'	69°38.0'	38	5.2	332	49	161	41	67	4
Nov. 12, 1972	17:56	38°20.0'	73°10.0'	111	5.9	125	44	332	44	229	14
Nov. 16, 1972	12:43	35°40.0'	69°55.0'	120	5.6	258	11	161	32	5	56
Dec. 3, 1972	8:54	39°22.0'	75°11.0'	64	5.0	359	24	100	24	230	56
Dec. 28, 1972	16:57	34°41.0'	70°22.0'	69	5.4	9	16	123	54	270	31
Jan. 12, 1973	23:39	36° 1.0'	70°40.0'	115	5.1	37	35	305	3	211	55
Jan. 19, 1973	15:10	32°45.0'	68°22.0'	38	4.7	119	78	339	10	247	8
Mar. 26, 1973	7:58	38°23.0'	73°56.0'	113	5.3	193	48	357	41	94	8
Apr. 25, 1973	3:16	37°40.0'	72°10.0'	114	5.3	112	2	19	66	203	24
Aug. 6, 1973	1:17	36°29.0'	70° 8.0'	218	5.1	107	3	200	41	13	49
Aug. 15, 1973	1:59	42°41.0'	67°25.0'	0	5.3	277	62	106	28	14	4
Oct. 17, 1973	3:16	36°23.0'	71° 7.0'	211	5.4	96	17	191	16	321	67

Table 1. List of earthquake mechanism solutions (continue)

Date	Origin Time	Lat. (°N)	Long. (°E)	Depth (km)	Mb	N-axes Az.	N-axes Pl.	P-axes Az.	P-axes Pl.	T-axes Az.	T-axes Pl.
Oct. 24, 1973	5:23	33° 9.0'	75°55.0'	37	5.3	234	49	103	30	358	25
Jan. 4, 1974	9:27	40°40.0'	77°40.0'	37	5.2	181	52	90	1	358	38
Feb. 20, 1974	11:43	40°39.0'	73°14.0'	49	4.8	43	34	311	4	216	56
Feb. 22, 1974	3:33	36°34.0'	71°29.0'	89	5.4	40	13	137	27	287	60
Apr. 6, 1974	20:19	37°11.0'	72°34.0'	45	5.2	103	71	342	10	249	16
Apr. 26, 1974	23: 0	35°55.0'	70° 5.0'	93	4.9	283	32	187	10	82	57
Mar. 13, 1974	17:40	36°32.0'	70°58.0'	197	5.3	46	37	158	26	274	42
Mar. 17, 1974	13:45	36°31.0'	70°57.0'	208	5.2	211	3	118	37	304	53
Jun. 3, 1974	11:45	36°53.0'	71°21.0'	105	5.2	247	23	339	4	79	67
Jun. 6, 1974	19: 3	36°25.0'	70°46.0'	212	5.1	41	2	132	34	309	56
Jul. 7, 1974	20:56	30°33.0'	78°29.0'	96	4.7	333	14	239	18	99	67
Jul. 30, 1974	5:12	36°25.0'	70°46.0'	210	6.3	160	39	255	6	353	51
Jul. 30, 1974	11:41	35°29.0'	71°28.0'	97	5.0	23	33	292	1	202	57
Aug. 11, 1974	5:12	39°20.0'	73°45.0'	48	5.3	51	27	142	3	238	63
Aug. 11, 1974	5:23	39°19.0'	73°45.0'	72	5.4	96	41	203	19	312	43
Aug. 11, 1974	20: 5	39°26.0'	73°40.0'	41	5.7	9	22	100	2	194	68
Sep. 29, 1974	15:51	40°18.0'	77°55.0'	24	5.3	293	35	24	1	116	55
Dec. 10, 1974	1:41	36°29.0'	70°28.0'	213	5.3	95	11	189	21	339	66
Dec. 28, 1974	12:11	35° 4.0'	72°55.0'	45	5.9	143	17	234	6	342	72
Dec. 30, 1974	4:47	36° 3.0'	69°43.0'	104	5.4	197	61	54	24	317	16
Jun. 19, 1975	8: 0	32°18.0'	78°40.0'	0	5.1	265	63	67	26	160	7
Jun. 19, 1975	8: 1	32°23.0'	78°30.0'	1	6.2	227	36	42	54	135	2
Jun. 19, 1975	8:12	31°56.0'	78°31.0'	49	5.8	338	69	248	0	158	21
Feb. 2, 1975	19:14	32°33.0'	78°30.0'	21	5.1	65	70	217	18	310	9
Feb. 11, 1975	20:30	38°35.0'	75°17.0'	27	5.0	22	19	289	8	176	70
Feb. 28, 1975	23:56	36°28.0'	70°42.0'	199	5.2	102	6	194	13	347	75
Mar. 3, 1975	9:48	36°27.0'	70°55.0'	187	5.3	50	13	318	9	193	74
Apr. 7, 1975	6:41	34°55.0'	72°58.0'	53	5.0	119	49	270	38	12	15
Apr. 9, 1975	22:25	37°60.0'	72°38.0'	107	5.3	221	30	349	48	113	27
Apr. 28, 1975	11: 6	35°48.0'	79°52.0'	0	5.8	299	73	213	1	123	18
Apr. 28, 1975	11:58	35°57.0'	79°58.0'	31	5.2	316	56	223	2	132	34
Apr. 29, 1975	3: 7	35°50.0'	79°53.0'	0	5.0	297	57	32	3	124	33
Jun. 4, 1975	2:24	35°50.0'	79°55.0'	0	5.6	356	38	163	51	261	6
Jul. 19, 1975	6:10	31°57.0'	78°35.0'	0	5.1	339	83	218	4	128	6
Jul. 29, 1975	2:40	32°34.0'	78°29.0'	0	5.5	178	56	352	34	84	3
Oct. 27, 1975	14:27	37°16.0'	78° 4.0'	22	4.8	39	53	291	13	192	34
Dec. 5, 1975	7:37	33° 6.0'	76° 8.0'	24	5.3	140	38	49	1	317	52
Dec. 11, 1975	10: 9	32°60.0'	76°10.0'	42	5.0	297	40	151	45	42	17
Jun. 7, 1976	0:24	32°58.0'	76° 7.0'	40	5.3	21	6	114	27	280	63
Mar. 19, 1976	13: 3	36°37.0'	67°46.0'	18	5.5	266	24	172	7	67	66
Jun. 11, 1976	5: 8	39°54.0'	77°17.0'	11	5.0	63	31	162	15	274	55
Jul. 10, 1976	10:21	39°17.0'	70°35.0'	39	5.1	173	30	29	55	273	17
Jul. 10, 1976	16:40	30° 2.0'	68°11.0'	7	5.2	291	30	194	11	86	58
Aug. 1, 1976	8:12	36°14.0'	68°37.0'	46	5.0	243	37	146	9	45	51
Aug. 3, 1976	7:50	40°49.0'	78° 0.0'	28	5.2	225	48	325	8	62	41
Sep. 3, 1976	21:52	38°54.0'	70°38.0'	22	5.1	234	34	143	3	49	56
Oct. 1, 1976	11:27	35°60.0'	77°27.0'	82	5.1	59	60	322	4	229	30
Oct. 20, 1976	10:37	38°38.0'	73°31.0'	93	5.1	209	66	349	18	84	14
Nov. 9, 1976	22:49	38° 7.0'	73°37.0'	152	5.2	132	58	323	32	230	5
Nov. 17, 1976	17:23	36°28.0'	71°11.0'	231	5.3	106	23	206	21	333	58
Nov. 27, 1976	21:42	36°31.0'	71° 3.0'	190	6.2	51	25	149	17	270	59
Jun. 7, 1977	6:31	34°37.0'	70°57.0'	48	5.1	97	35	229	45	347	26
Jun. 31, 1977	14:26	40° 7.0'	70°52.0'	20	6.0	55	11	324	6	206	77
Feb. 12, 1977	4:49	37° 7.0'	71°14.0'	86	5.3	288	50	174	19	70	34
Feb. 14, 1977	0:22	33°36.0'	73°16.0'	27	5.2	157	68	11	19	277	11
Feb. 27, 1977	9:21	38° 4.0'	72°43.0'	107	5.1	32	64	125	2	216	26
Apr. 13, 1977	11:33	36°28.0'	70°52.0'	195	5.1	47	35	156	24	273	45
Apr. 18, 1977	0:13	36°26.0'	70°46.0'	215	5.3	52	24	150	17	271	60
Mar. 4, 1977	2:37	36°58.0'	71°27.0'	102	5.0	274	41	174	12	70	46
Jun. 3, 1977	2:31	36°25.0'	70°46.0'	207	5.4	131	11	223	8	350	76
Jun. 22, 1977	15:53	33°11.0'	76° 2.0'	47	4.9	295	41	142	46	37	14
Jul. 18, 1977	14:22	35°31.0'	70° 6.0'	72	5.2	314	16	179	67	49	15
Jul. 29, 1977	9:14	38°13.0'	75°11.0'	114	5.3	187	49	84	12	344	39
Sep. 12, 1977	9:33	37° 4.0'	67°17.0'	21	4.9	126	26	360	50	231	28
Nov. 15, 1977	20:20	38°13.0'	74°11.0'	157	4.7	25	43	258	33	147	29
Dec. 6, 1977	10:52	41°33.0'	69°43.0'	25	5.2	64	18	156	7	267	70
Dec. 18, 1977	16:47	39°52.0'	77°18.0'	21	5.3	43	15	136	9	255	73
Dec. 25, 1977	16:18	38°53.0'	70°41.0'	7	5.3	245	52	142	10	44	36
Jan. 16, 1978	3:20	36°25.0'	70°44.0'	214	5.2	92	33	195	19	310	50
Mar. 12, 1978	8:29	41°55.0'	79°58.0'	19	5.3	65	32	159	5	257	57
Mar. 24, 1978	21: 5	42°50.0'	78°36.0'	34	6.1	297	10	206	2	107	80
Apr. 14, 1978	6:11	41° 6.0'	75°22.0'	38	5.1	39	56	158	18	258	28
Apr. 21, 1978	15:22	36°38.0'	71°16.0'	230	5.8	349	14	89	36	241	51
Mar. 7, 1978	10:32	33°24.0'	73°38.0'	25	5.0	160	65	264	7	357	24
Jun. 14, 1978	16:12	32°14.0'	76°37.0'	7	5.0	118	71	265	16	358	10
Oct. 23, 1978	8: 7	36°29.0'	70°57.0'	183	5.6	260	2	351	17	163	73
Nov. 1, 1978	19:48	39°20.0'	72°34.0'	7	5.9	137	73	320	18	50	1
Nov. 2, 1978	6:24	39°21.0'	72°40.0'	1	5.3	72	73	303	11	211	13
Nov. 7, 1978	3: 4	37°14.0'	71°49.0'	123	5.1	101	48	247	37	351	18
Nov. 8, 1978	0:57	39°19.0'	72°35.0'	36	5.4	47	19	314	10	198	69
Apr. 17, 1979	17: 1	38°34.0'	73°28.0'	95	5.1	278	37	175	16	66	48
Jun. 26, 1979	3: 4	36°28.0'	71°14.0'	229	5.7	84	9	175	5	293	80
Aug. 14, 1979	14:24	36°29.0'	70°54.0'	189	5.1	126	6	217	11	8	77
Aug. 20, 1979	3:50	36°29.0'	70° 9.0'	231	5.9	270	70	176	26	15	63
Feb. 13, 1980	22: 9	36°28.0'	76°52.0'	74	6.0	294	12	197	29	43	58
Apr. 14, 1980	10:17	36°23.0'	69°35.0'	40	5.3	5	3	274	18	103	72
May. 10, 1980	11:23	30° 1.0'	68°14.0'	0	5.0	77	68	244	21	336	5
Jul. 5, 1980	20:25	41°55.0'	77°25.0'	22	5.4	28	12	120	12	256	73
Jul. 18, 1980	6: 5	36°38.0'	71°23.0'	178	5.1	167	9	73	26	275	62
Aug. 23, 1980	21:36	32°58.0'	75°45.0'	3	5.2	304	37	193	27	76	42
Sep. 19, 1980	9:30	36°25.0'	70°46.0'	209	5.3	302	22	206	12	89	64
Dec. 11, 1980	14:35	41°20.0'	69° 7.0'	14	5.0	107	58	291	32	200	2

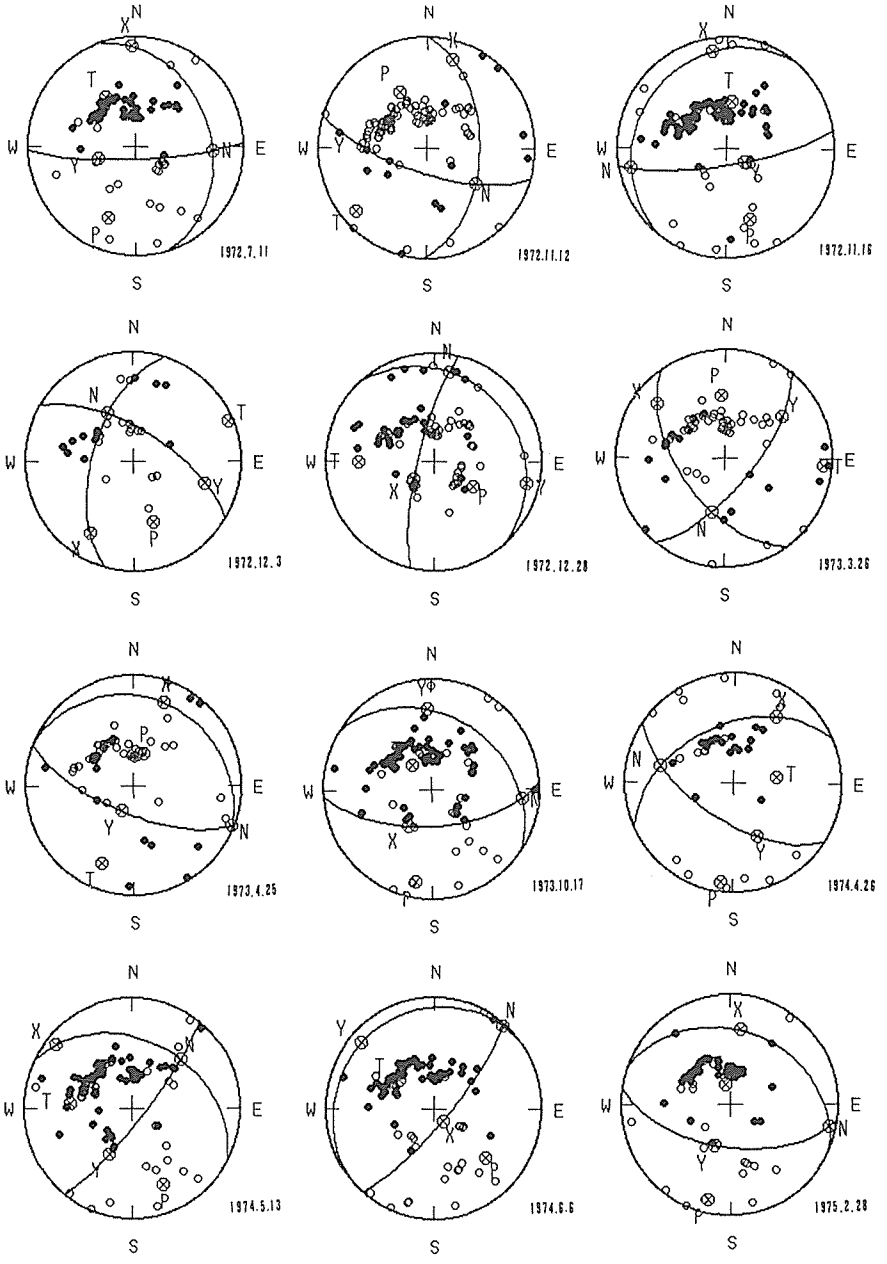
1972.7.11
1972.11.12
1972.11.16
1972.12.3
1972.12.28
1973.3.26
1973.4.25
1973.10.17
1974.4.26
1974.5.13
1974.6.6
1975.2.28

Fig. 2. (a)

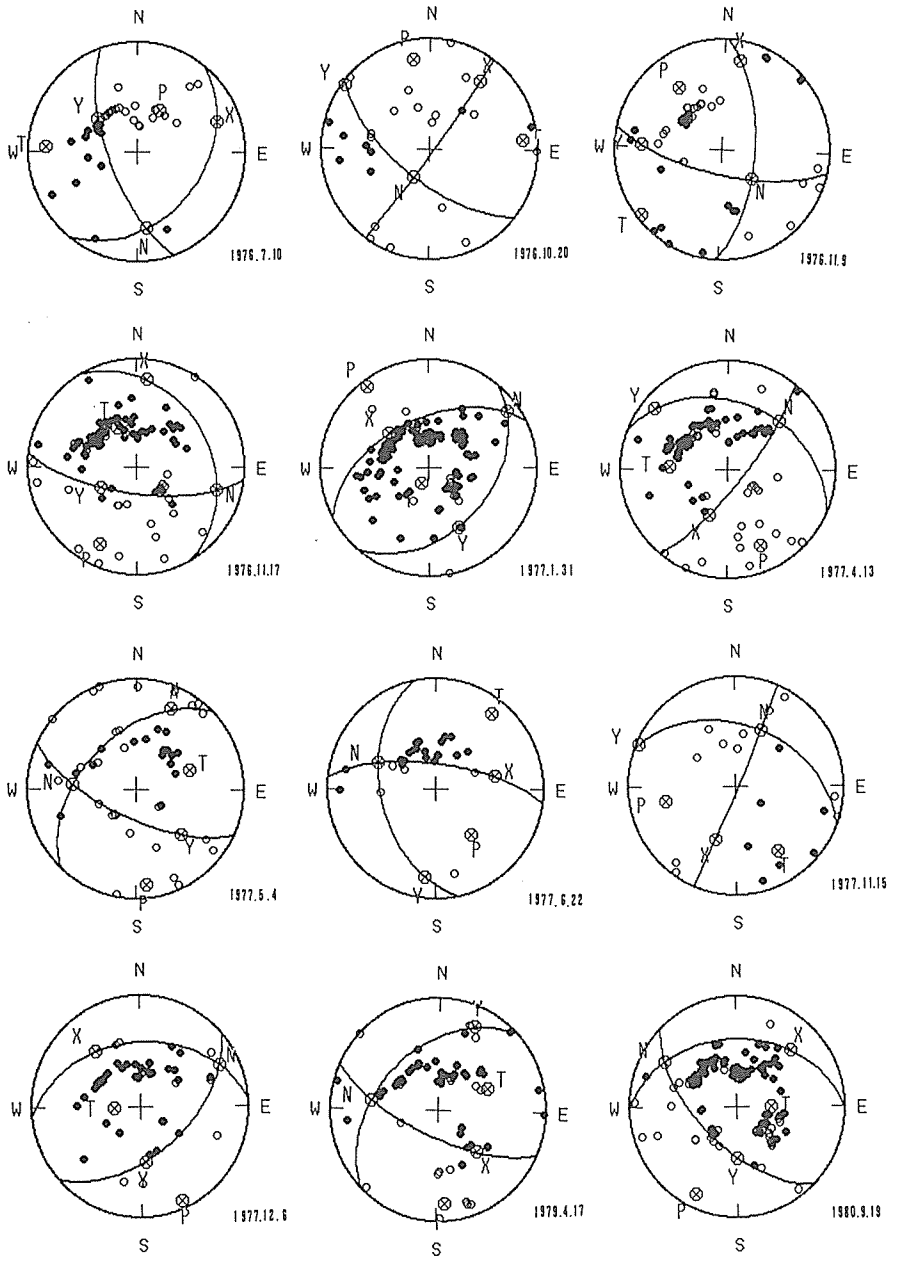

Fig. 2. (b)

Fig. 2. Typical mechanism solutions and P wave first motion data in the form of the Wulff's net projection (lower hemisphere) of 24 earthquakes determined in this study. Closed and open circles indicate the compressions and dilatations, respectively.

selected from the Bulletins and focal mechanism solutions were determined. We used accurate mechanism solutions of 119 earthquakes in and around the Hindukush-Pamir region to discuss the characteristics of tectonics. Magnitudes (Mb) of these 119 earthquakes are in the range from 4.7 to 6.3. Their depths are in the range from the surface to 231 km. We added 11 focal mechanism solutions during the same period determined by Xu et al. (1988). These 130 solutions are shown in Table 1. Typical Wulff's net projections of 24 new mechanism solutions are shown in Fig. 2.

Average azimuths and plunge angles of the principal compressive (P-axes) and the tensile axes (T-axes) for various depths in each region have been calculated by the smoothed radiation pattern method similar to that introduced by Oike (1971). At first, the typical directions of P- and T-axes in each region were determined from the distribution of them on the Wulff's net. The numbers of the P-axes (Np) and the T-axes (Nt) within an angular distance of 45° from 61 reference points uniformly covering on the surface of hemisphere were counted for each point. Then a normalized parameter K was calculated by

$$K = (Np - Nt)/N$$

where $N = (Np + Nt)$ is the total number of used data. After parameters K for the 61 points are obtained, points with the maximum K value and the minimum K value were determined. Average azimuth and plunge angle of P- and T-axes were calculated from the distribution of P- and T-axes on the half space whose center is the point with the maximum K and minimum K.

3. Spatial distribution of the directions of P-, T-axes and the null vector (N-axes)

3.1. Shallow earthquakes with depths from 0 to 70 km

Shallow earthquakes with depth less than or equal to 70 km occurred widely in the Hindukush-Pamir region and its surroundings. The distribution of the earthquakes whose mechanism data are used and five regions divided for this study are shown in Fig. 3. The regions are the western Hindukush region (A1), the Pamir and the western part of the South Tianshan region (A2), the eastern part of the South Tianshan region (A3), the western Himalayan and the Kashmir region (A4), and the southern Hindukush region (A5). There are few shallow earthquakes and many intermediate depth earthquakes in the southern Hindukush region (A5). The horizontal components of P-axes and T-axes of the focal mechanism solutions of shallow earthquakes distribute as shown in Fig. 4 and Fig. 5, respectively. The P-axes in the three regions (A1, A2, A3) mainly lie in the NWN-SES direction. To the contrary, almost all of the P-axes lie in the NE-SW direction in the western Himalayan and the Kashmir region (A4). The T-axes have small horizontal components in the NE-SW direction in the former three regions (A1, A2, A3). The horizontal T-axes lie in the NW-SE direction in the western Himalayan and the Kashmir region (A4). The region A5 seems to be a transition zone between the regions A1 and A4, where there are both P-axes with NE-SW and NW-SE directions,

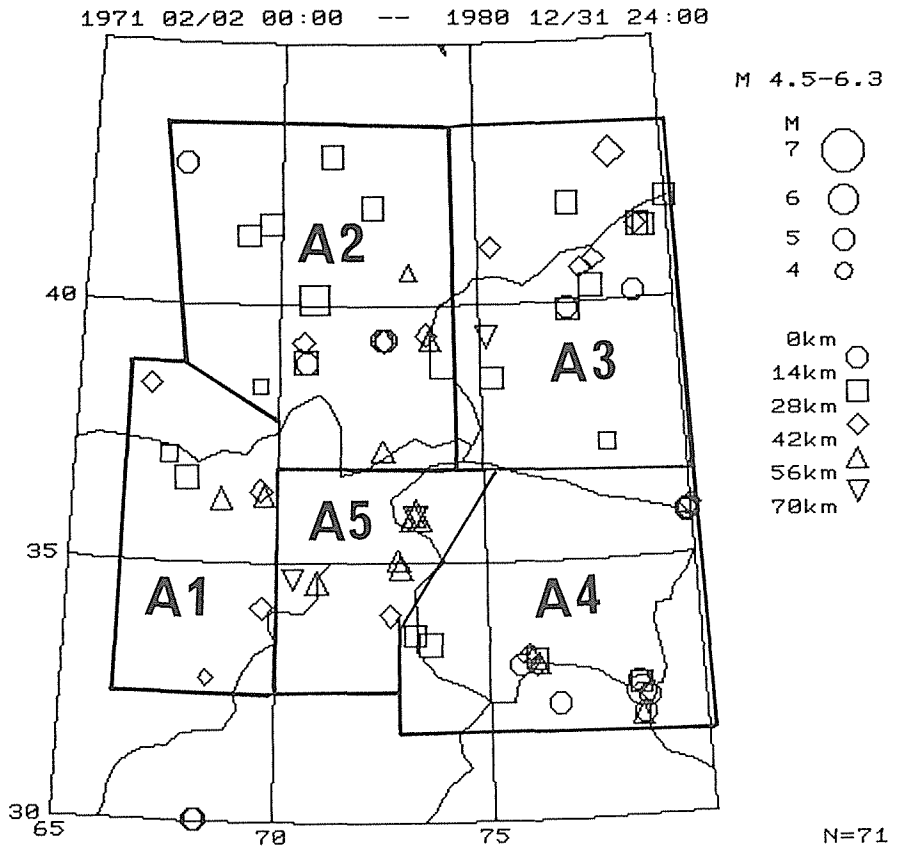

Fig. 3. Epicentral distribution of shallow earthquakes (depth range from 0 km to 70 km) whose mechanism solutions were used in this paper and five regions: A1, A2, A3, A4 and A5 correspond to A1; the western Hindukush region, A2; the Pamir and western part of the South Tianshan region, A3; the eastern part of the South Tianshan region, A4; the western Himalayan and the Kashmir region, and A5; the southern Hindukush region, respectively.

and the T-axes with variant directions, too. To observe the regional characteristics in detail, the P-, T- and N-axes in each region were projected on the Wulff's net. The distribution of the P-, T- and N-axes in each region are shown in Fig. 6. Circles, squares and triangles in Fig. 6 represent the projections of P-, T- and N-axes on the Wulff's net, respectively. Fig. 6 shows that most P-axes lie horizontally in the NWN-SES direction and that horizontal components of T-axes lie in the NE-SW direction in A1 and A2 regions. It means that the horizontal compressional force in the NWN-SES direction is dominating the stress field in the western Hindukush region (A1) and the Pamir and the western part of the South Tianshan region (A2). The horizontal compression in NW-SE direction and the vertical extension are dominant in the eastern part of the South Tianshan region (A3). It means that many thrust type faulting events are occurring here. The diagrams of P-, T- and N-axes in the western Himalayan and Kashmir region (A4)

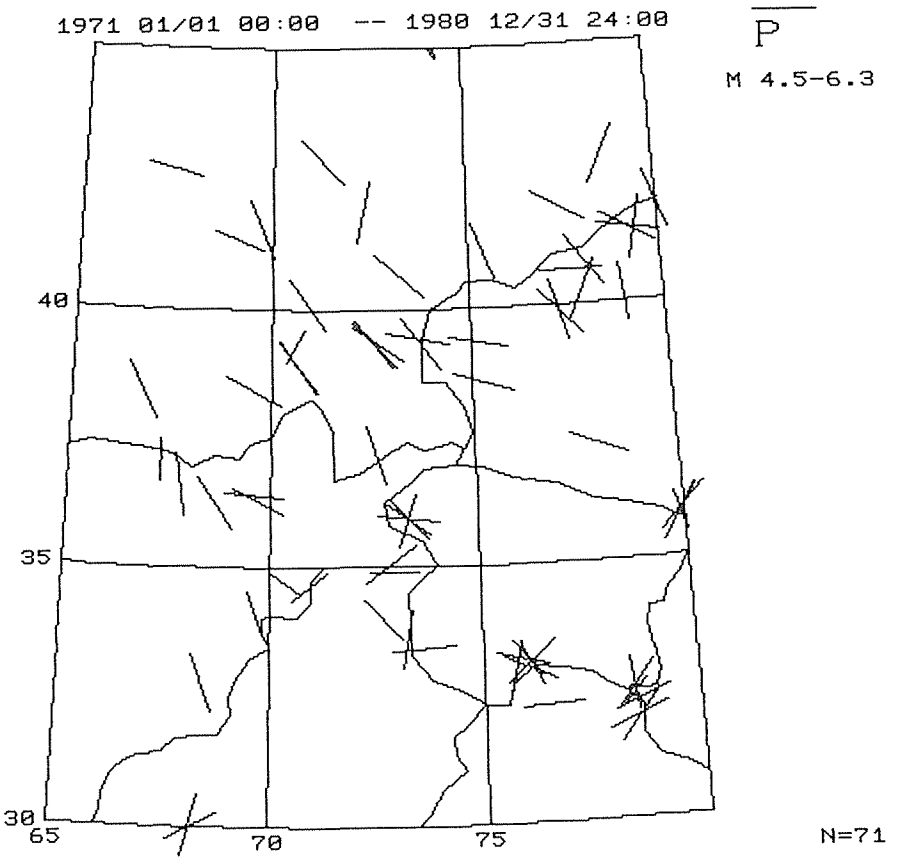

Fig. 4. Horizontal projection of compressional axes (P-axes) of shallow earthquakes (depth range from 0 km to 70 km) shown in Fig. 3.

show the different pattern from those of the three regions mentioned above. Most P- and T-axes lie in the NE-SW and NW-SE direction, respectively. The crustal stress field in this region is characterized by the horizontal NE-SW compression and the horizontal NW-SE extension. The directions of P- and T-axes in the region A5 show that the region is a transition region between the region A1 and the region A4.

3.2. Intermediate depth earthquakes with depths from 71 to 240 km

Intermediate depth earthquakes in the Hindukush-Pamir region occurred in the depth from 71 km to about 240 km during the period from 1971 through 1980. They are divided into three groups with various depths as follows.

3.2.1. The events with depths from 71 km to 100km

The distribution of earthquakes with depths from 71 km to 100 km is different from that of shallow earthquakes. They are mainly concentrated into two regions

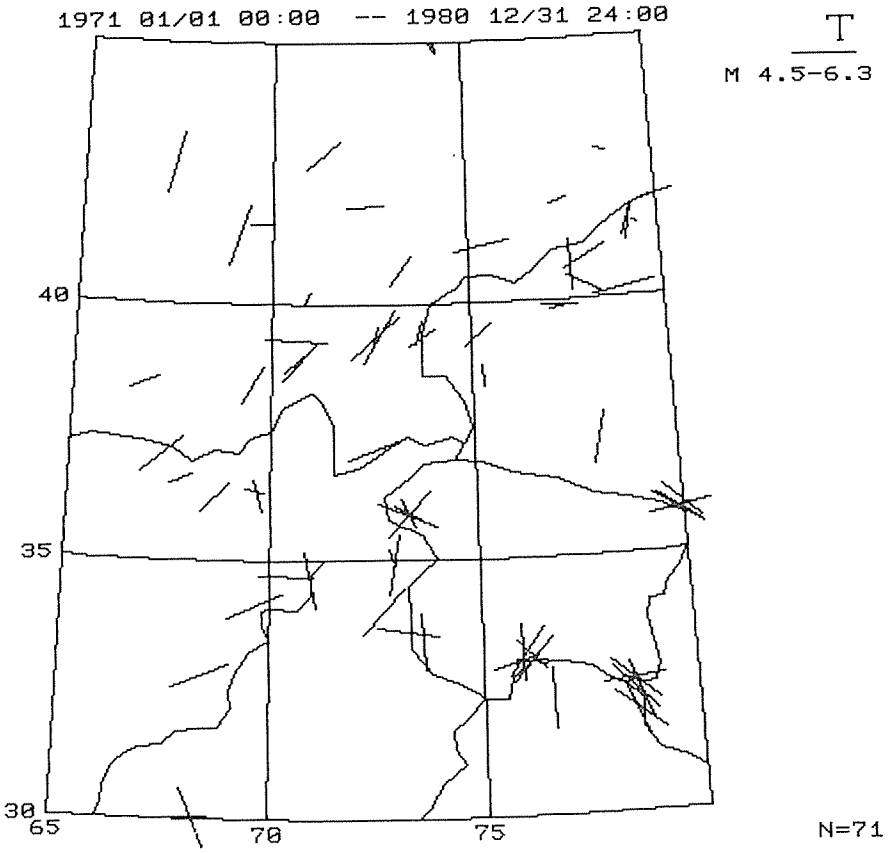

Fig. 5. Horizontal projection of extensional axes (T-axes) of shallow earthquakes (depth range from 0 km to 70 km) shown in Fig. 3.

as shown in Fig. 7. One is the eastern Hindukush region (Fig. 7, B1) and another is the western part of South Tianshan region (Fig. 7, B2). P- and T-axes of focal mechanism solutions of earthquakes with depths from 71 to 100 km are shown in Fig. 8 and Fig. 9, respectively. The diagrams of P-, T- and N-axes in the two regions are shown in Fig. 10.

Most of P-axes lie in the NW-SE direction or in the N-S direction in the eastern Hindukush region (B1). Most of T-axes expect three lie in the vertical direction there. P-axes in the western part of the South Tianshan region (B2) lie in the N-S direction. T-axes mainly lie in the WNW-ESE direction there (Fig. 9). The results shown in Fig. 10 indicate that the stress field in the depth from 71 to 100 km in the eastern Hindukush region (B1) is mainly dominated by the horizontal compression in the NW-SE direction and the extension in vertical cirection. However, the stress field is characterized by the horizontal compression in the N-S direction and the extension in the WNW-ESE direction in the western part of the South Tianshan region (B2).

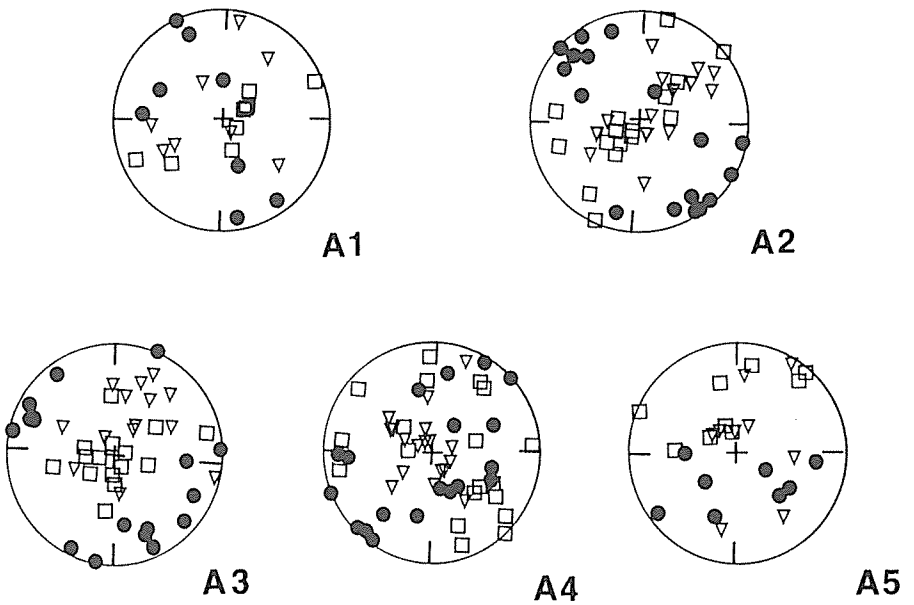

Fig. 6. Distribution of P-axes (circles), T-axes (squares) and N-axes (triangles) of shallow earthquakes, the (a), (b), (c), (d) and (e) correspond to the regions A1, A2, A3, A4 and A5 shown in Fig. 3, respectively.

3.2.2. The events with depths from 101 km to 170 km

Earthquakes from 101 km to 170 km deep reveal the belt-like distribution with the NE-SW trend from the Pamir region to the eastern Hindukush region. They can be divided into two regions as shown in Fig. 11. One is the eastern Hindukush region (C1) and another is the Pamir region (C2). Fig. 12 and Fig. 13 show the horizontal projections of the P- and T-axes of focal mechanism solutions of events in Fig. 11, respectively.

Most of the P-axes in the eastern Hindukush region (C1) lie in the N-S direction and the P-axes in the Pamir region (C2) lie in the NW-SE direction (Fig. 12). The horizontal components of T-axes in the eastern Hindukush region (C1) are shorter than those of P-axes. It means that the T-axes have large vertical components. Most of T-axes in the Pamir region (C2) lie in the NEN-SES direction (Fig. 13). Fig. 14 shows the diagrams of the P-, T- and N-axes in two regions shown in Fig. 11. In the eastern Hindukush region (C1), most P-axes are near N-S direction and have small plunge angles. T-axes lie approximately in the vertical direction there. The result shown in Fig. 14 indicates that the stress field in this range in the eastern Hindukush region is formed by the compressional stress in the N-S direction and the vertical extensional stress. It means that reverse dip-slip faultings occur there. In the Pamir region (C2), P-axes lie in the WNW-ESE direction or near to the vertical. Most T-axes in this region lie in the NE-SW direction. The stress field in the depth range from 101 km to 170 km in the Pamir region (C2) is different with those in the eastern Hindukush region (C1).

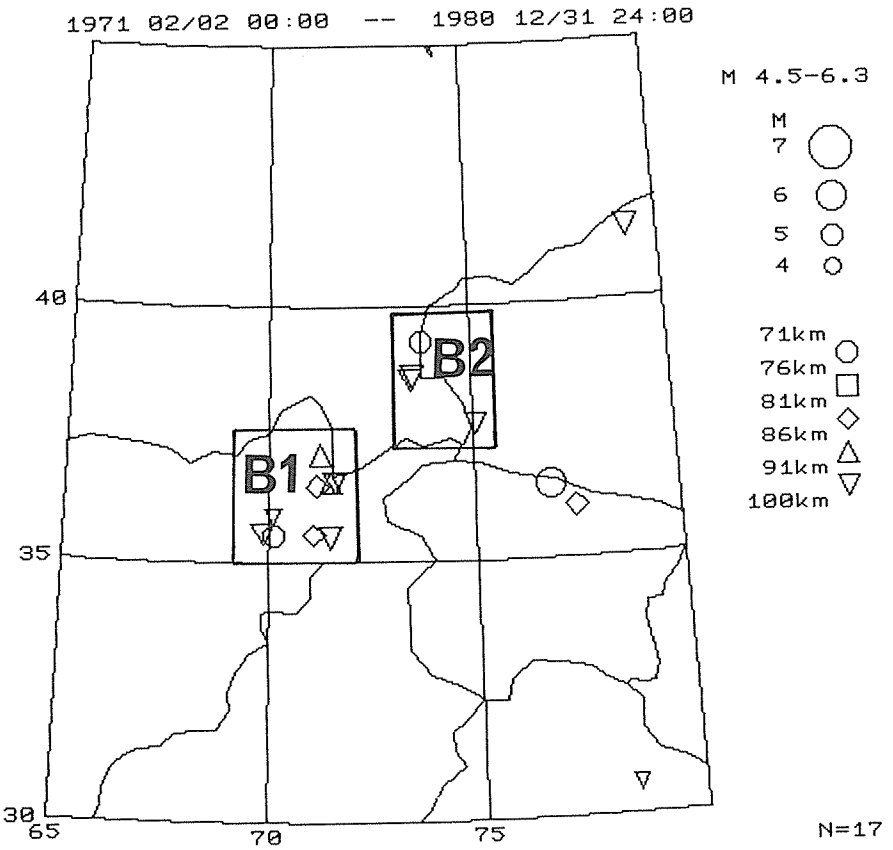

Fig. 7. Epicentral distribution of intermediate depth earthquakes with depth range from 71 km to 100 km. B1; the eastern Hindukush region, B2; the western part of the South Tianshan region.

3.2.3. The events with depths from 171 km to 240 km

The deepest seismic zone in the Hindukush-Pamir region is found in the depth range from 171 km to 240 km. The epicenters of all events with depths from 171 km to 240 km concentrate into the small area under the eastern part of the Hindukush region (Fig. 15). The P- and T-axes of focal mechanisms are shown in Fig. 16 and Fig. 17, respectively. Their diagrams of P-, T- and N-axes are shown in Fig. 18.

Although the directions of horizontal projection of P-axes in Fig. 16 seem to be scattered, the P-axes mainly lie in the N-S direction. The lengths of horizontal projection of T-axes are obviously shorter than those of P-axes. The regional stress field is analyzed from the diagram of P, T and N-axes of all focal mechanisms as shown in Fig. 18. Most P-axes distribute horizontally in the N-S or the NW-SE directions. Almost all of T-axes lie in the vertical direction. The N-axes are in the horizontal direction. This result indicates that the vertical extension force in this deepest zone is so strong that many reverse faulting events occurred here. The

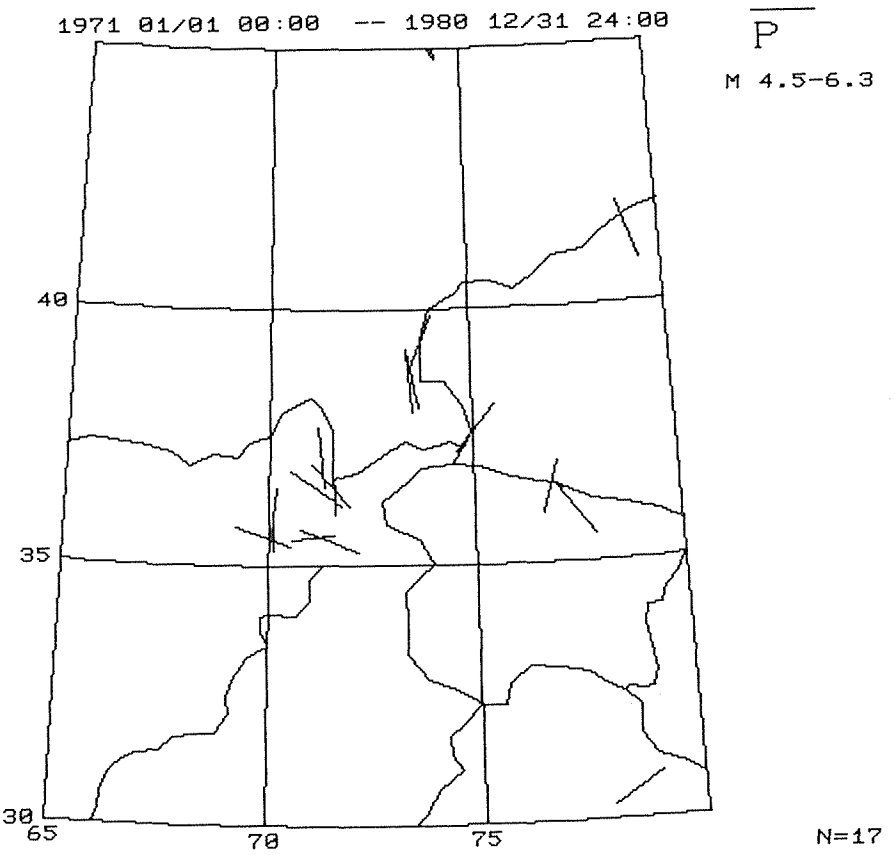

Fig. 8. Horizontal projections of P-axes of intermediate depth earthquakes with depth range from 71 km to 100 km shown in Fig. 7.

vertical tensile stress play an important role in the occurrence of the reverse faulting events there.

According to the results above mentioned, regional average values of the azimuth and plunge angle of P- and T-axes of focal mechanism solutions in various depths in the Hindukush-Pamir region are summarized in Table 2, except the A5 region where the axes do not concentrate. Regions in Table 2 correspond to those in Figs. 3, 7, 11 and 15. The K values correspond to the maximum K in the smoothed radiation pattern, which represent the concentrativeness of the axes. Regional concentrativeness of T-axes is generally better than that of P-axes in the Hindukush-Pamir region, especially in the intermediate depth seismic zone. It implies that the tensile stress is a significant seismogenic force in this region.

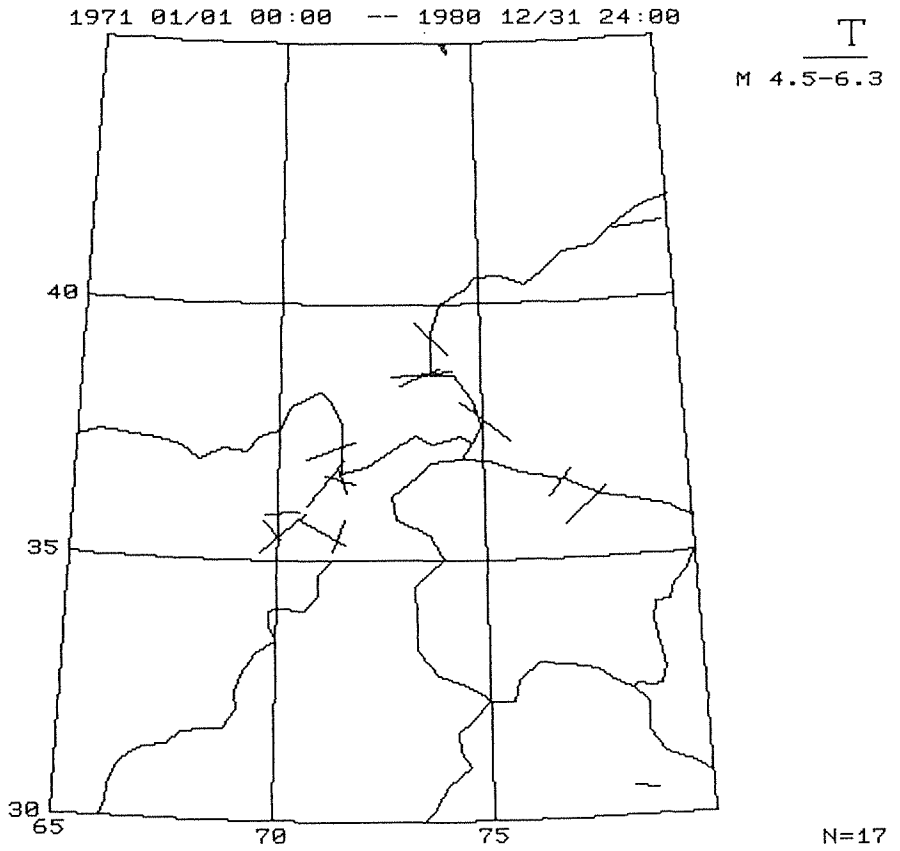

Fig. 9. Horizontal projections of T-axes of intermediate depth earthquakes with depth range from 71 km to 100 km shown in Fig. 7.

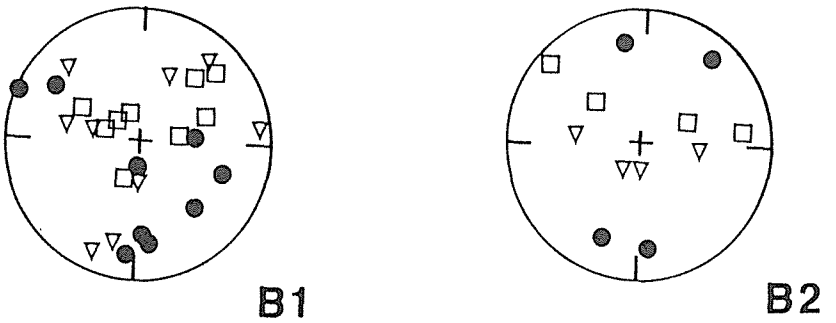

Fig. 10. Distribution of P-axes (circles), T-axes (squares) and N-axes (triangles) of intermediate depth earthquakes in the regions B1 and B2 shown in Fig. 7.

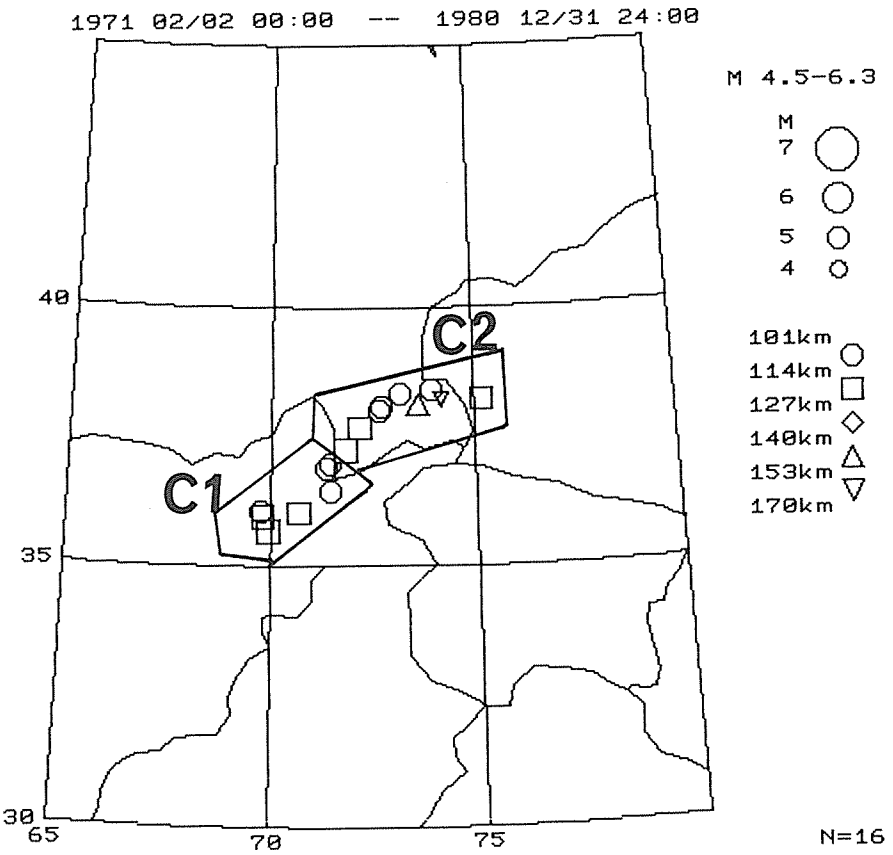

Fig. 11. Epicentral distribution of intermediate depth earthquakes with depth range from 101 km to 170 km. C1; the eastern Hindukush region, C2; the Pamir region.

4. Earthquake faulting types in each depth

Characteristics of the distribution of earthquake faulting types in different depths are discussed on basis of the distribution of directions of the P-, T- and N-axes shown in the former section. In order to clarify the characteristics of the distribution of the earthquake faulting types, earthquakes were classified into three types as follows. If the plunge angle of the P-axis of a focal mechanism is larger than that of its T-axis, and if it is equal to or more than 40°, the earthquake is regarded to be caused by the dislocation of normal fault and is classified into the group of the normal faulting type earthquake. In the same way, if the plunge angle of the T-axis is large than that of its P-axis, and is equal to or more than 40°, the earthquake is classified into the group of the reverse faulting type. If both the plunge angle of the P- and T-axis are less than 40°, the earthquake is classified into the strike-slip faulting type. We use this classification of earthquake faulting types to clarify characteristics of the stress field in the Hindukush-Pamir region. In

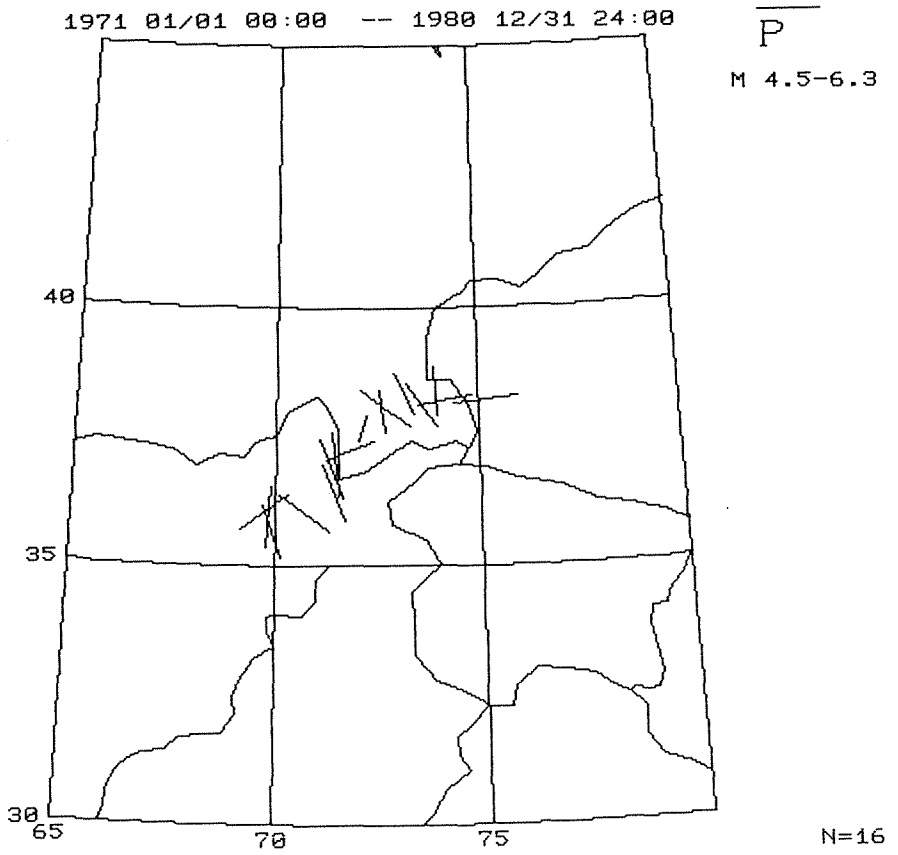

Fig. 12. Horizontal projections of P-axes of intermediate depth earthquakes with depth range from 101 km to 170 km shown in Fig. 11.

Fig. 19, (a), (b), (c), (d) and (e) show the distributions of the reverse, normal and strike-slip fault type earthquakes in each depth. All focal mechanism solutions of 130 earthquakes determined by authors are used. Open circles, closed circles and crosses in Fig. 19 represent the normal, the reverse and the strike-slip faulting type events, respectively.

Shallow events (depth range from 0 km to 29 km) did not occur in the area just above the intermediate depth earthquake zone. Many reverse faulting events occur in the Pamir and the South Tianshan regions in the northern side of the intermediate earthquake zone in the Hindukush-Pamir region (Fig. 19, (a)). It is noticeable that some normal faulting events occurred in the depth range from 30 km to 82 km in the area south of the intermediate depth earthquake zone in the Hindukush-Pamir region (Fig. 19, (b)). The depths of these five normal faulting type events are 38 km, 48 km, 69 km, 72 km and 82 km from the south to the north. They seem to become deeper from the south to the north. There are some reverse faulting events in the South Tianshan region in the depth range from 30

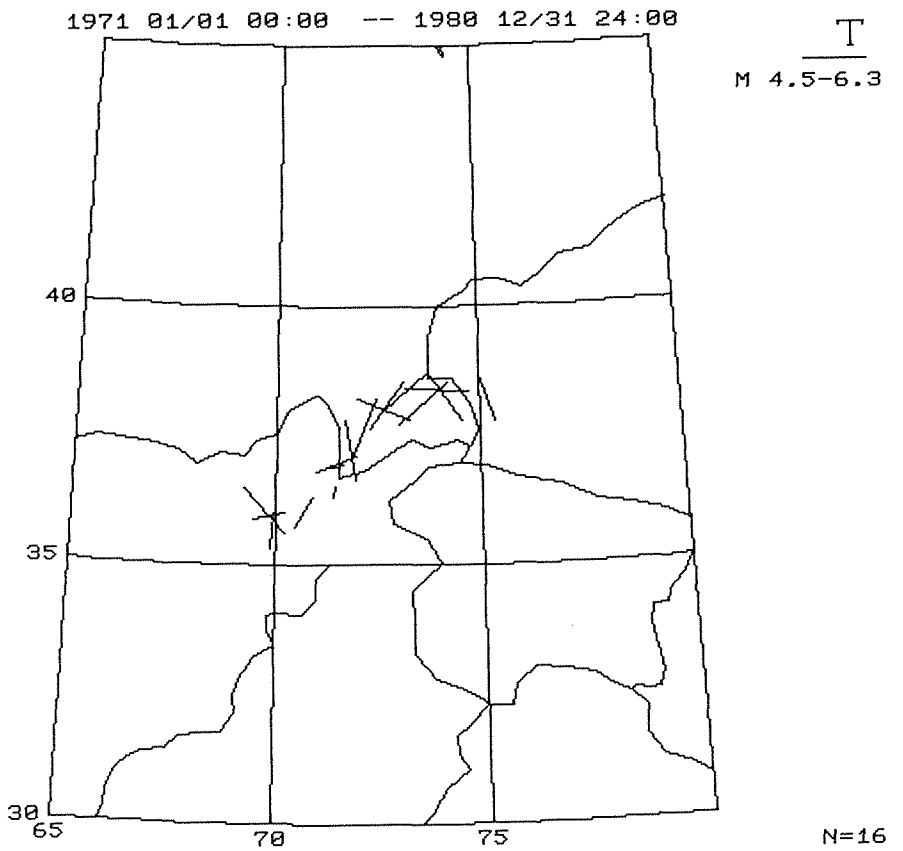

Fig. 13. Horizontal projections of T-axes of intermediate depth earthquakes with depth range from 101 km to 170 km shown in Fig. 11.

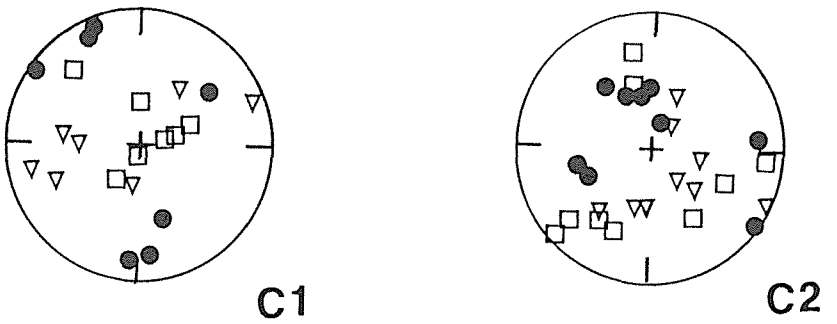

Fig. 14. Distribution of P-axes (circles), T-axes (squares) and N-axes (triangles) of intermediate depth earthquakes in the regions C1 and C2 shown in Fig. 11.

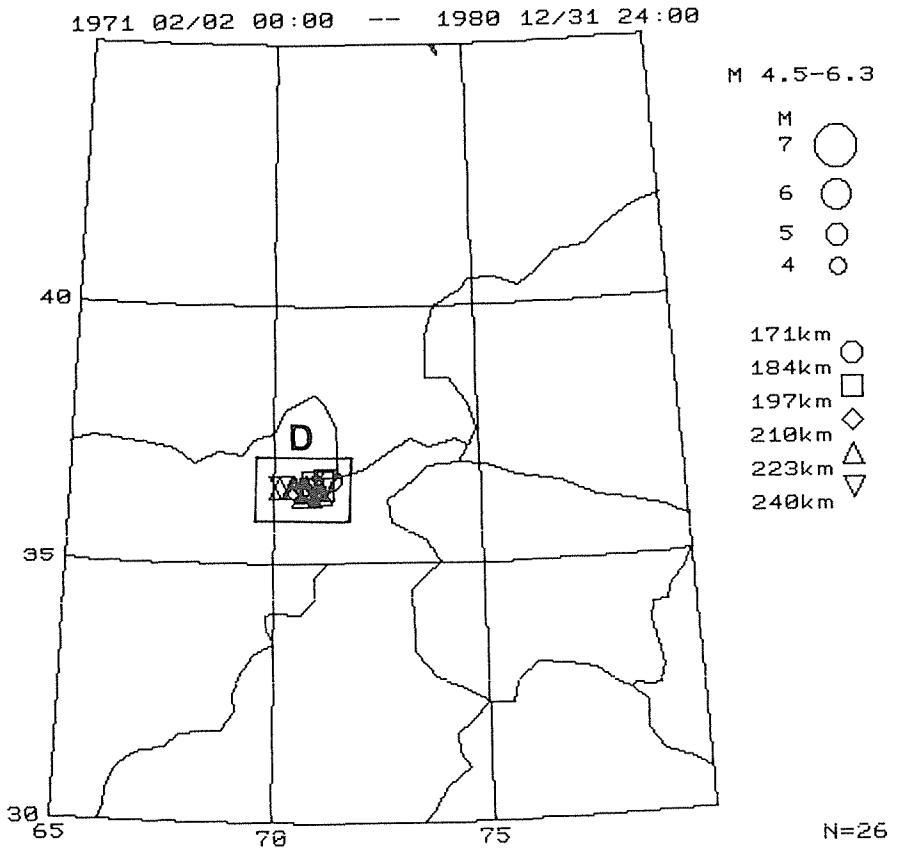

Fig. 15. Epicentral distribution of the intermediate range earthquakes with depth range from 171 km to 240 km, which are concentrated in the eastern part of the Hindukush region.

km to 82 km (Fig. 19, (b)). The reverse faulting events in the depth range from 83 km to 99 km (Fig. 19, (c)) concentrate to the intermediate depth earthquake zone of the Hindukush-Pamir region. Earthquakes in the depth range from 100 km to 170 km distribute along the narrow belt with NE-SW trend (Fig. 19, (d)). The earthquake faulting type in the northeastern part (the Pamir region) of the belt-like distribution is different with those in its southwestern part (the eastern Hindukush region). There are some normal and strike-slip faulting events only in the Pamir region. All reverse faulting events in this depth range are in the eastern Hindukush region. All earthquakes from 171 to 240 km deep concentrate at the eastern Hindukush region. All of them are reverse faulting type events. Epicentral distribution reveals a belt-like trend in the E-W direction (Fig. 19, (e)).

From these results, the regional characteristics of focal mechanisms in various depths in the Hindukush-Pamir region are summarized as follows.

(1). There are mainly two kinds of the shallow stress field in depth range from the surface to 70 km in the Hindukush-Pamir region. The P-axes are

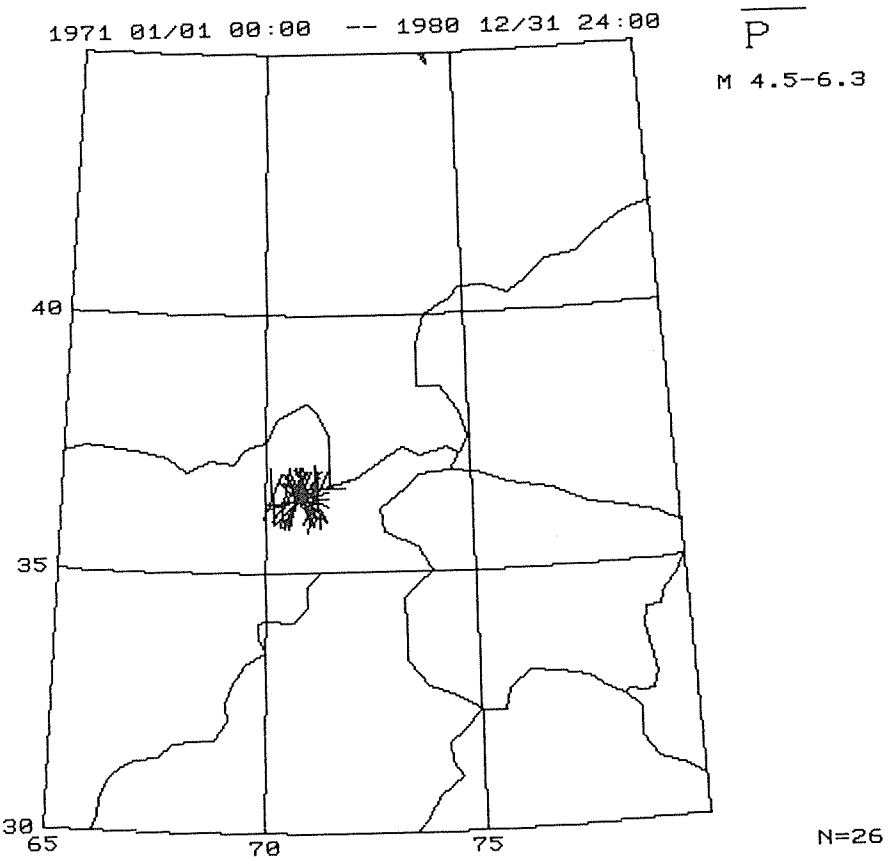

Fig. 16. Horizontal projections of P-axes of intermediate depth earthquakes with depth range from 171 km to 240 km shown in Fig. 15.

horizontal in the NWN-SES direction and the T-axes are vertical in the western Hindukush, the Pamir and the South Tianshan regions (A1, A2 and A3) located north or northwest of the boundary segment between the Indo-Australian and Eurasian plates in this region. However, the P- and T-axes are horizontal in the NE-SW and NW-SE directions in the western Himalayan and Kashmir region (A4) which is near to the eastern part of this boundary segment. There are many reverse fault type events in the western Hindukush, Pamir and South Tianshan regions (A1, A2 and A3) and strike-slip type events in the western Himalayan and Kashmir region (A4). Some normal faulting events concentrate only in the region located in south of the Hindukush intermediate depth earthquake zone (A5).

(2). The epicentral distribution in the Hindukush-Pamir region becomes the more concentrative in the small area the deeper from surface to about 240 km. The deepest part of the intermediate depth zone with near E-W trend is located under the eastern Hindukush. Most of them are reverse faulting type events. P-axes of the intermediate depth events have the horizontal N-S direction which coincide

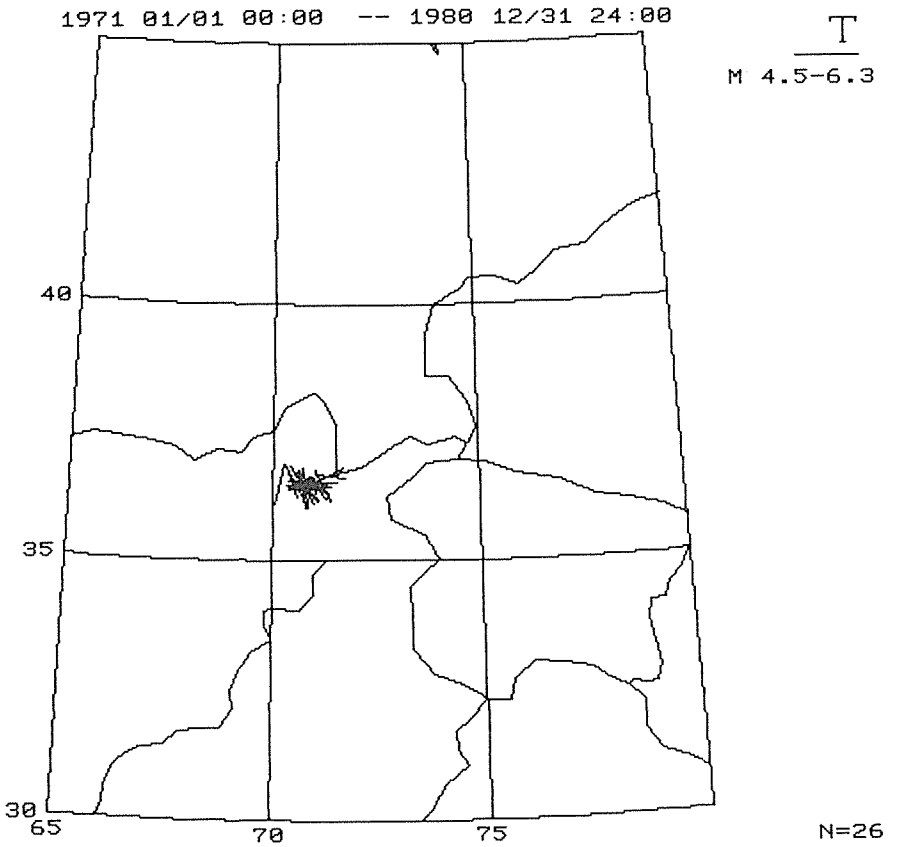

Fig. 17. Horizontal projections of T-axes of intermediate depth earthquakes with depth range from 171 km to 240 km shown in Fig. 15.

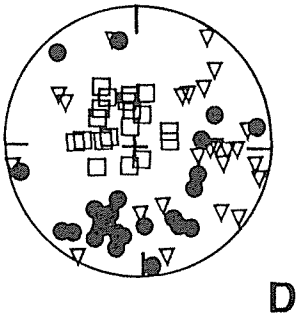

Fig. 18. Distribution of P-axes (circles), T-axes (squares) and N-axes (triangles) of intermediate depth earthquakes with depth range from 171 km to 240 km shown in Fig. 15.

Table 2. The regional average values of the directions and the plunge angles of the P-axes and T-axes in various depths. Azi. and Plu. mean the azimuths and plunge angles, and the K means the K value, respectively.

Depth (km)	Regions	P-axes			T-axes		
		Azi.	Plu.	K	Azi.	Plu.	K
0-70	A1	322.6	33.9	0.46	63.2	15.5	0.58
	A2	149.8	27.2	0.50	52.5	22.3	0.56
	A3	157.0	34.7	0.53	243.8	35.3	0.68
	A4	223.6	44.2	0.23	132.3	45.9	0.26
71-100	B1	139.8	33.6	0.50	249.8	30.3	0.50
	B2	191.8	20.8	0.50	282.8	28.5	0.50
101-170	C1	169.1	26.7	0.47	103.3	46.8	0.73
	C2	311.9	36.5	0.56	203.8	45.3	0.44
171-240	D	185.7	41.6	0.62	280.3	44.8	0.96

nearly to the direction of the relative motion between the Indo-Australian plate and the Eurasian plate. T-axes in the deep zone concentrate in the vertical direction. The hyposentral distribution of earthquakes from the southern shallow zone to the northern intermediate depth zone seems to configure a slab of the plate subduction.

5. Distribution of focal mechanisms along the N-S profile through the intermediate depth earthquake zone

In order to investigate the seismo-tectonics of the intermediate depth earthquake zone and generation of stress field in the intermediate and shallow parts in Hindukush-Pamir region, the vertical section along longitudinal AB line shown in Fig. 20 is shown in Fig. 21. The width of projected zone is equal to the width of the intermediate depth earthquake zone under the Hindukush region. The 54 shallow and intermediate depth events are shown in Fig. 21. The hypocentral distribution in the longitudinal profile seems to form a sinking seismic belt from south to north. There are two seismic gaps in the distribution. One of them is in the crust located to the north of the Hindukush intermediate depth earthquake zone. The another gap is located around 160 km deep along the Hindukush intermediate depth earthquake zone (Chatelain et al., 1980).

Earthquake faulting types along the profile are also shown in the Fig. 21. Open circles, closed circles and triangles represent the normal, the reverse and the strike-slip faulting events, respectively. It is noticeable in Fig. 21 that there is not only the sinking seismic belt of the subduction zone from the south to the north,

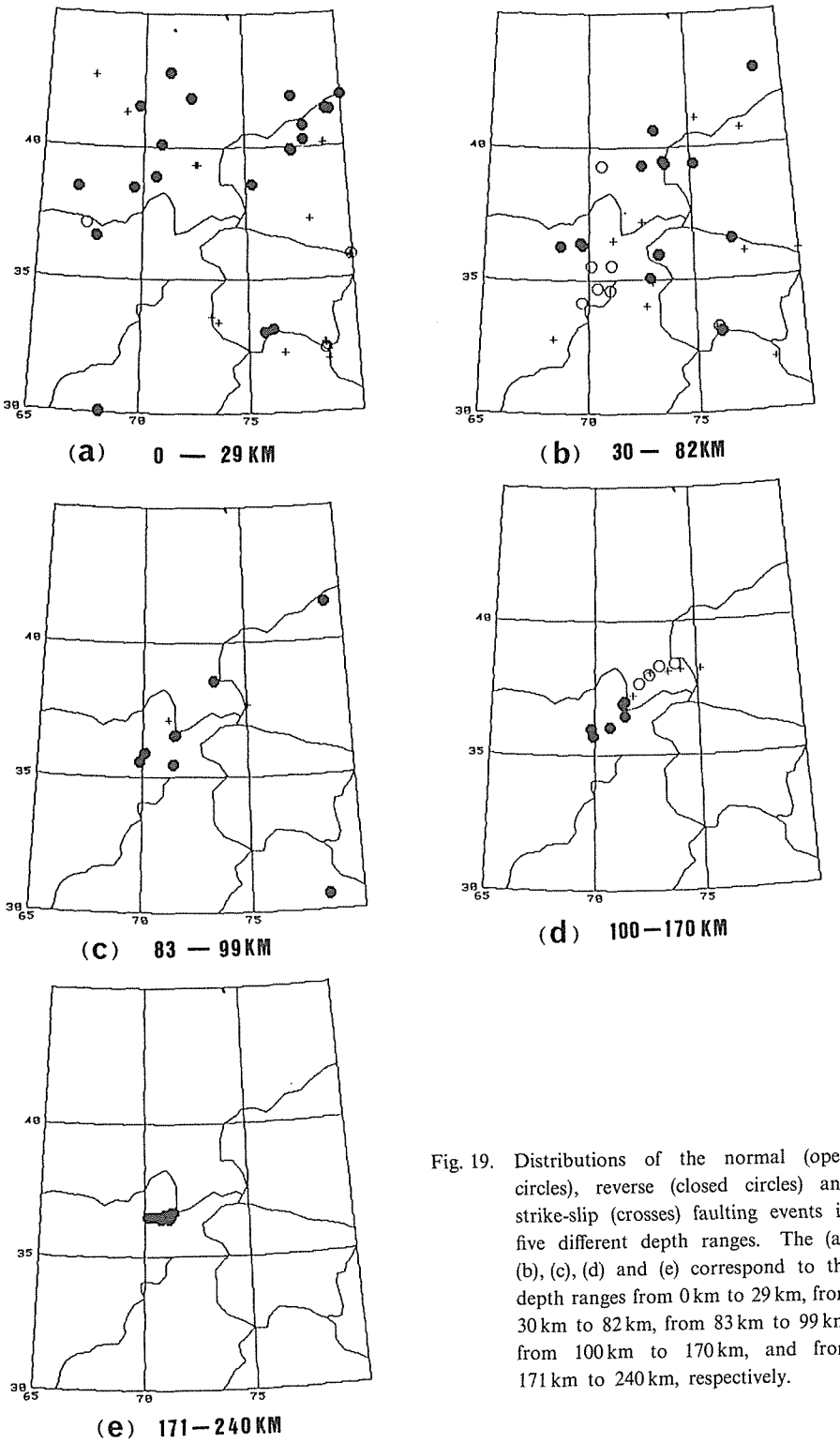

Fig. 19. Distributions of the normal (open circles), reverse (closed circles) and strike-slip (crosses) faulting events in five different depth ranges. The (a), (b), (c), (d) and (e) correspond to the depth ranges from 0 km to 29 km, from 30 km to 82 km, from 83 km to 99 km, from 100 km to 170 km, and from 171 km to 240 km, respectively.

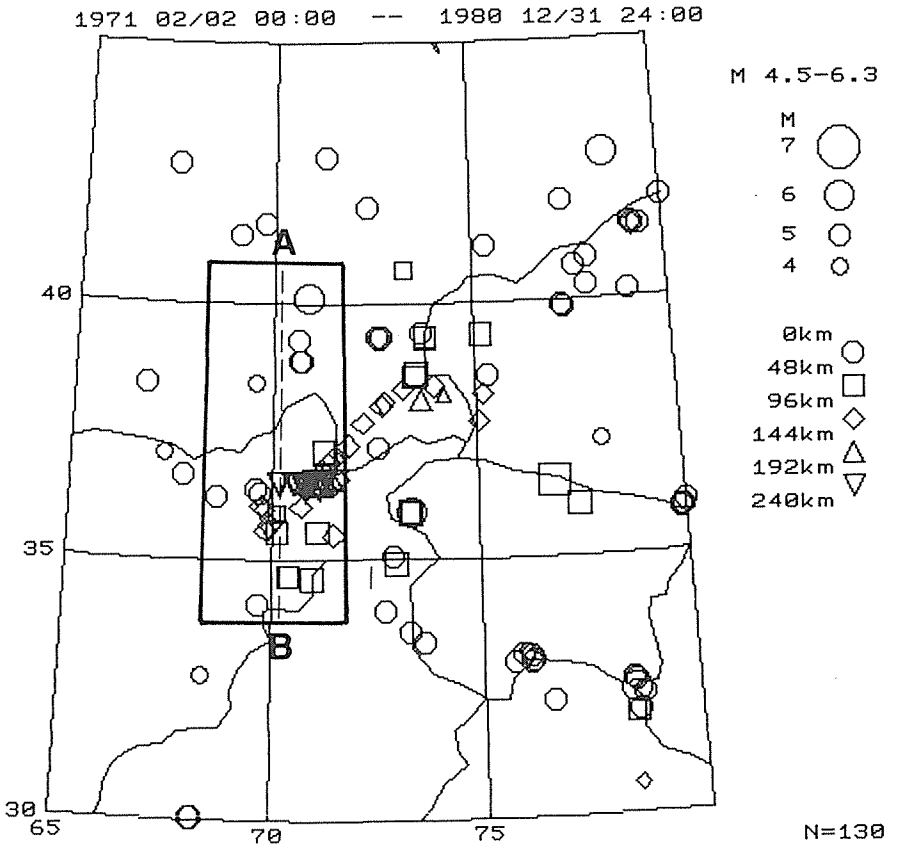

Fig. 20. Epicentral distribution of all shallow and intermediate depth earthquakes. The profile along AB in the Hindukush-Pamir regions shown in Fig. 21.

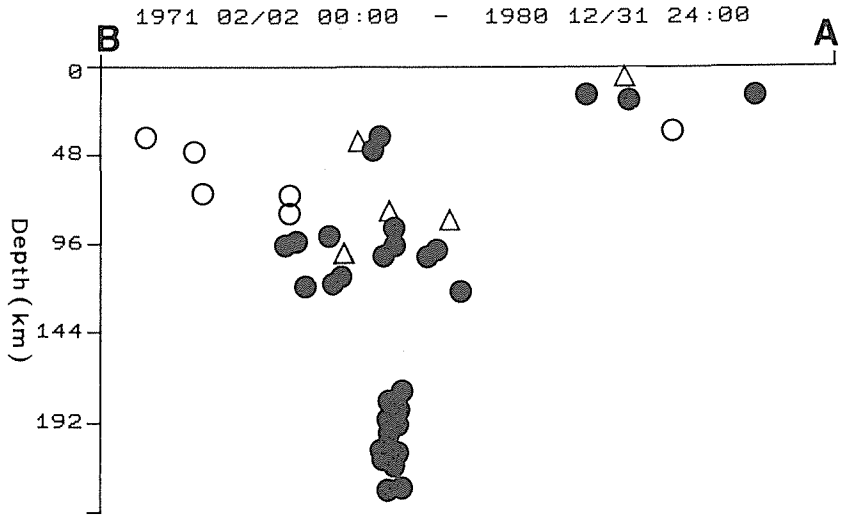

Fig. 21. Longitudinal profile through the Hindukush intermediate depth earthquake zone. Open circles, closed circles and triangles correspond to normal, reverse and strike-slip faulting events, respectively.

but also there is a significant change of distribution for the normal, strike-slip and reverse faulting types from the southern shallow part to the northern deep part. In the shallow part of the sinking seismic belt with the depth between 38 km and 82 km, only some normal faulting earthquakes occurred along the subduction with low angle. Strike-slip and reverse faulting events concentrated in the depth from 82 km to 130 km in the intermediate depth part where the sinking seismic belt begins to turn into vertical direction. There is a seismic gap in the depth about 160 km. The gap separates the sinking seismic belt into two parts. A lot of reverse faulting events are concentrated in the deepest part of the sinking seismic belt with depth from 178 km to 231 km along the vertical direction. Few strike-slip faulting type events occurred here, and normal faulting type events did not occur in this deepest part.

The sinking seismic belt in the profile AB in Fig. 20 from the south to the north under the Hindukush region is similar to some slabs of subducting plate (Suyehiro et al., 1986). In order to have a better understanding of the seismo-tectonics here, the profile maps of the projections of P- and T-axes of focal mechanisms along AB in Fig. 20 are shown in Figs. 22 (a) and (b), respectively. In Figs. 22 (a) and (b), the solid line means that the line is outward, and the dotted line means that the line is inward, respectively. Fig. 22 (a) indicates that the directions of P-axes are perpendicular to the sinking seismic zone. As shown in Fig. 22 (b) there is the stress field that T-axes are parallel to the sinking seismic zone. This is a very instructive distribution for understanding the tectonics in the Pamir-Hindukush region. Oliver et al. (1973) pointed out that four types of the distributions of stress field within slabs in the world. One of them is the down-dip extension stress field. The distribution of stress within the slab in the Hindukush-Pamir region as mentioned before is the down-dip extension stress field. Such characteristics on stress field in the Hindukush sinking seismic belt are similar to the stress field of down-dip extension type of a slab which penetrates into the asthenosphere in some other subduction zones (Oliver et al., 1973; Bannister et al., 1989). So, it can be concluded that there exists a subduction zone of the southern Indo-Australian plate under the northern Eurasian plate in the Hindukush-Pamir region.

As for the Pamir region located to the northeast of the intermediate depth earthquake zone of the eastern Hindukush region, the deepest earthquakes occurred about 150 km deep. The distribution pattern of the stress there is different from that in the Hindukush region. The P-axes of focal mechanism solutions of shallow and intermediate depth earthquakes lie in the NW-SE direction. Some normal faulting events are in the deeper part and their T-axes lie in the NE-SW direction. Such a stress field may be caused by the pull force from the deepest part in the eastern Hindukush region which is located to the southwest of the Pamir region.

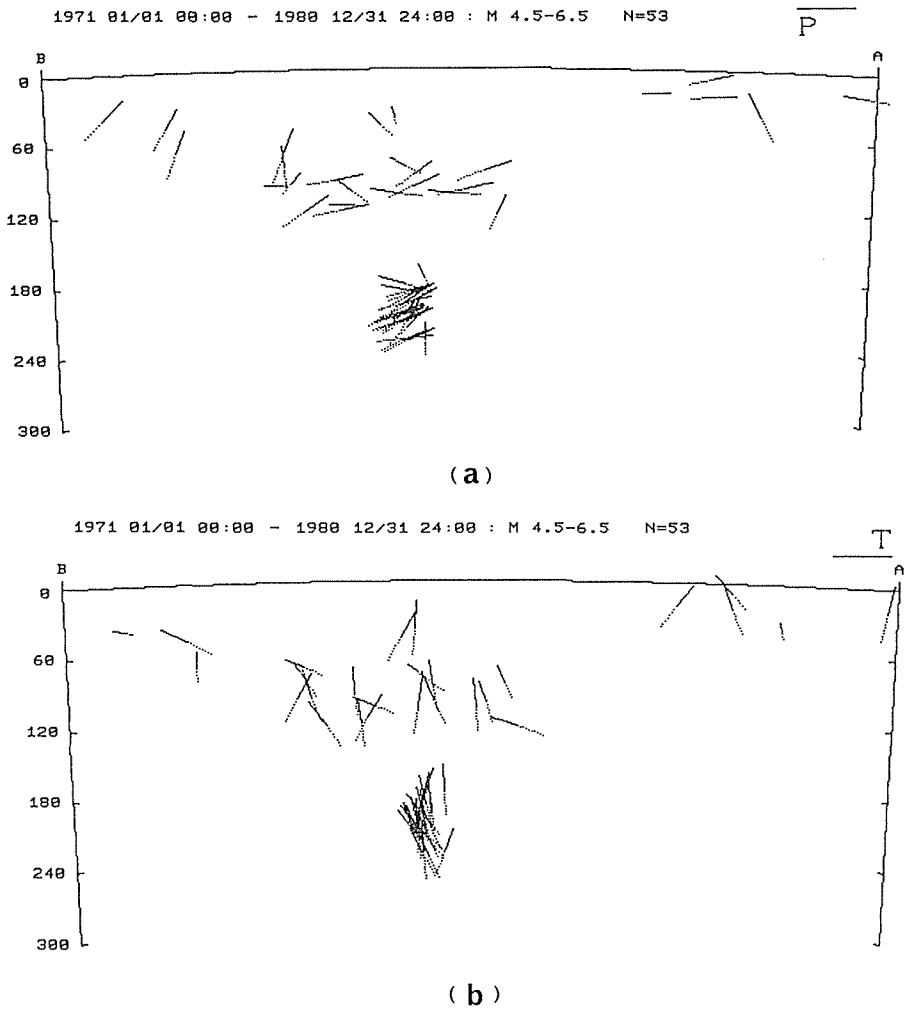

Fig. 22. Longitudinal profile of P-axes (a) and T-axes (b) through the south Hindukush intermediate depth earthquake zone. Solid and dotted lines show the outward and the inward directions, respectively.

6. The subduction zone and its tectonic implication in Hindukush-Pamir region

According to the epicentral distribution and the focal mechanism solutions in the Hindukush-Pamir region shown in Fig. 21 and Figs. 22 (a) and (b), it can be said that there is a narrow subduction zone of the Indo-Australian plate to the Eurasian plate. According to the results obtained in this study, the schematic seismotectonic map in the Hindukush-Pamir region is illustrated in Fig. 23. The large arrow indicates the relative motion direction of the Indo-Australian plate to the Eurasia plate in the Hindukush-Pamir region. The small arrows mean the compressive direction of the stress field in and around the Hindukush-Pamir region.

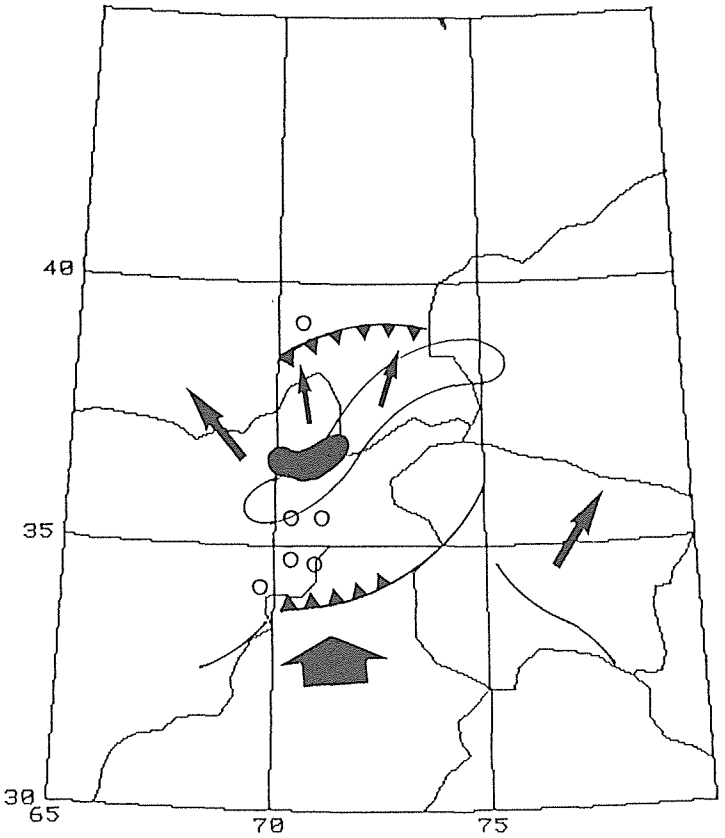

Fig. 23. Schematic tectonic map in and around the Hindukush-Pamir region. Large arrows show the relative movement direction of the Indo-Australian plate to the Eurasian plate. Small arrows show the compressive direction of the crustal stress field in the Hindukush-Pamir region. Open circles mean the normal faulting shallow events (depths < 83 km). Open area and closed area mean the intermediate depth earthquake zones with depth ranges from 101 km to 170 km and from 171 km to 231 km, respectively..

The boundary between two plates and major faults in this region were also shown in Fig. 23. Fig. 24 shows the schematic map along the profile through the intermediate depth earthquake zone. Open and closed circles correspond to the discribution ranges of the normal and reverse faulting events, respectively. The other arrows mean the relative motion direction between the slab and the block or between the block and fault, respectively. The Indo-Australian plate moving toward the Eurasian plate is reaching far into the north in the Pamir region and is penetrating into the Eurasian plate like a wedge. A narrow belt subducts under the Eurasian plate in the Hindukush region. The collisions between these two plates exist in both the western and eastern sides of the narrow subduction zone in Hindukush.

Based on the results in this study, the Indo-Australian plate encounters with the Eurasian plate at about 34°N and begins to subduct at the northern boundary

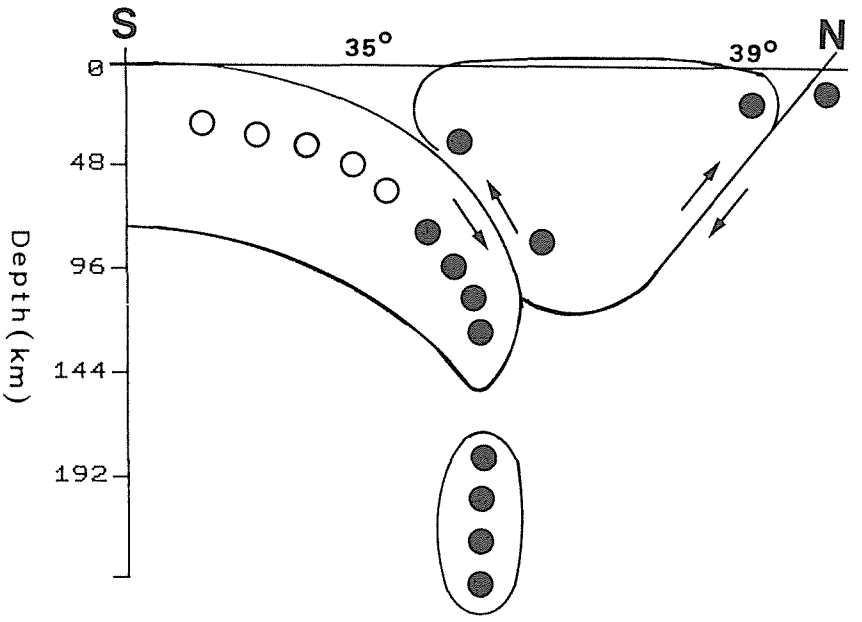

Fig. 24. Schematic tectonic implications of longitudinal profile through the Hindukush intermediate depth earthquake zone. Arrows mean the relative movement directions between the slab and the block or between the block and the fault. Open and closed circles correspond to the distribution ranges of the normal and reverse faulting events, respectively.

beneath the Hindukush mountains. Normal fault events occur in the shallow slab segment inclining with a low angle between 34°N and 35.5°N by the effect of pull force from the deeper subducting plate. When the slab sinks down into the intermediate depth part and turns to the vertical direction, the strike-slip and reverse fault events occur in the segment of slab from 83 km to 130 km deep. There is a seismic gap about 160 km deep and it divides the slab into two parts. This may be because that the lower portion of slab is sinking more rapidly and had been parted from the higher portion of the slab sith the slower sinking velocity. A lot of reverse faulting events have occurred here between about 35.5°N to 36.5°N with depth from 170 km to 240 km. Although the faulting type of events changes from the normal type to the reverse type, the P-axes always are perpendicular to the slab, and the T-axes are within the slab and parallel to the inclination direction of the slab. This indicates that the pull force along the subduction zone by its own weight is dominant. Although the deepest part of subduction zone in the Hindukush region is about 260 km deep, the deepest part of the slab is still in the asthenosphere (Jordan, 1979) and it does not reach to the resistance from the mesosphere with relative strength and viscidity.

The motion of the subduction zone of the Indo-Australian plate moving toward the Eurasian plate in the Hindukush-Pamir region produces the great influence on the crustal stress field in its surroundings. The northward drift like a wedge of

the subduction zone is obstructed by the blocks to north of the Hindukush region. Therefore, the N-S compression in the intermediate depth seismic zone is produced. The lateral ejection acting for the crust of its eastern and western blocks is produced. This structure and movement make the direction of compressive stress in the western and eastern parts change towards the west and east from the north direction. There is a crustal stress field with the NWN-SES compression in the western Hindukush, Pamir and the South Tianshan regions, which are located in the north and the west of the subduction zone in the Hindukush-Pamir region. Crustal stress field with the NE-SW compression and NW-SE extension is acting in the western Himalayan and the Kashmir region which is located in the east to the subduction zone. The lateral ejections are caused by the compressional stress field to the both sides of the northwest and northeast directions (see Fig. 23).

The Indo-Australian plate is moving towards the Eurasian plate at rate of 4.5 cm/year in the Pamir region (Minster et al., 1974). The direction of compressional stress in the Hindukush is about 174° near N-S based on the result from the present research. This direction approximates that of relative movement between the plates in the Hindukush region. The tectonic force from the Indo-Australian plate causes the northern block to go up along the fault and many shallow events with thrust faulting to occur along the south Tianshan seismic region (Fig. 23, Fig. 24). The shallow seismic gap between the Hindukush intermediate earthquake zone and the shallow seismic belt in the Pamir region (see Fig. 23, Fig. 24) may be related with the existence of strong blocks.

7. Conclusions

(1) There is the subduction zone of the Indo-Australian plate moving towards to the Eurasian plate in the eastern Hindukush region. The deepest earthquake in the subduction zone is about 260 km deep. There is a distribution of stress field with the down-dip extension within the Hindukush subduction zone, where P-axes are perpendicular to the slab and T-axes are parallel to the inclination of the slab.

(2) The northward drift of the Hindukush subduction zone causes the compression in the N-S direction in the intermediate depth segment and the lateral ejection in the crust. It generates the stress fields as P-axes with the NWN-SES direction in the Hindukush, Pamir and South Tianshan regions which are located to the north and the west of the Hindukush subduction zone, and P-axes with the NE-SW direction in the Himalayan and Kashmir regions which are located to the east of the Hindukush subduction zone.

(3) The tectonic force from the subduction motion makes the shallow block to the north of the Hindukush upthrust along the thrusting faults. So a shallow seismic gap is formed in the region to the north of the Hindukush subduction zone and many shallow reverse faulting events occur in the Pamir region.

Acknowledgments

The authors thank Dr. Kazuo Matsumura for providing valuable data and his kind helps. We would like to thank to Dr. Keiko Kuge for her fruitful discussions. We would also thank Mr. Yuzo Ishikawa for providing his program for this study. Data were processed on the FACOM M340R of the Information Data Procession Center for Disaster Prevention Research, Disaster Prevention Research Institute, Kyoto University.

References

Bannister, S.C., Perin, B.J. and Webb, T.H., 1989, Normal faulting through subducted oceanic crust: the 19 July 1985 earthquake of Hawke's Bay, New Zealand, Tectonophysics, **162**: 303–313.

Chatelain, J.L., Roecker, S.W., Hatzfeld, D. and Molnar, P., 1980, Microearthquake seismicity and fault plane solutions in the Handu Kush region and their tectonic implications, J. Geophy. Res., **85**: **B3**, 1365–1387.

Gansser, A., 1977, The great suture zone between Himalaya and Tibet–A preliminary account. Himalaya, Sciences de la Terre, Centre National de la Recherche Scientifique, Paris, 209–212.

Jordan, T.H., 1979, The deep structure of the continents, Scientific American, **240**: 1, 70–82.

Kakkuri, J. and Konttinen, R., 1986, Surface deformations in Central Asia, Tectonophysics, **130**: 333–336.

Khalturin, V.I., Rautian, T.G. and Molnar, P., 1977, The spectral content of Pamir-Hindu kush zone in the upper mantle, J. Geophys. Res., **82**: **20**, 2931–2943.

Minster, J.B., Jordan, T.H., Molnar, P. and Haines, E., 1974, Numerical Modeling of Instantaneous Plate Tectonics, Geophys. J. R. Astr. Soc., **36**: 541–576.

Ni, J. and M., Barazangi, 1984, Seismotectonics of the Himalayan Collision Zone: Geometry of the Underthrusting Indian Plate Beneath the Himalaya, J. Geophys. Res., **89**, B2, 1147–1163.

Ning, J.Y, and S.X. Zang, 1990, The distribution of earthquakes and stress state in Pamir-Hindukush regions, Acta Geophysica Sinica, **33**, **6**, 657–669 (in Chinese).

Oike, K., 1971, On the natural of the occurrence of intermediate and deep earthquakes. 1. The world wide distribution of the earthquake generating stress, Bulletin of the Disaster Prevention Research Institute, Kyoto University, **20**: 145–182.

Oliver, J., Isacks, B., Barazangi, M. and Mitronovas, W., 1973, Dynamics of the down-going lithosphere, Tectonophysics, **19**: 133–147.

Santo, T., 1969, Regional study on the Characteristic Seismicity of the World, Part 1, Hindu kush Region, Bull. Earthq. Inst., Tokyo Univ., **47**: 1035–1048.

Roecker, S.W., Soboleva, O.V., Nersesov, I.T., Lukk, A.A., Hatzfeld, D., Chatelain, J.L. and Molnar, P., 1980, Seismicity and fault plane solutions of intermediate depth earthquakes in the Pamir-Hindu kush region, J. Geophys. Res. **85**: **B3**, 1358–1364.

Sugi, N. and Kikuchi, M., 1990, Earthquakes and tectonics in the collision zone, Programme and Abstracts, Seismological Society of Japan, No. 2, 160 (in Japanese).

Suyehiro, K. and Asada, T., 1986, The subduction of plate and deep earthquakes, The formation of the Japanese Islands–It's history and the present as a mobile belt–edited by Daira A. and Hagamura I., 24–31 (in Japanese).

Verma, R.K. and Sekhar Chandra C., 1985, Seismotectonics and focal mechanisms of earthquakes from Pamir-Hindukush regions, Tectonophysics, **112**: 297–324.

Vinnik, L.P., Lukk, A.A. and Nersesov, I.L., 1977, Nature of the intermediate seismic zone in the mantle of Pamir-Hindukush, Tectonophysics, **38**: T9–T14.

Xu, J.R., Zhao, Z.X., Ishikawa, Y. and Oike, K. 1988, Properties of the stress field in the around West

China derived from earthquake mechanism solutions, Bull. Disas. Prev. Res. Inst., Kyoto Univ., Vol. 38, Part 2, **No. 333**, 49–78.

Zhao, Z.X., Matsumura, K., Oike, K. and Ishikawa, Y., 1988, Regional characteristics of temporal variation of seismic activity in East Asia and their mutual relations, (3) West China and its neighboring regions, Zisin, **41**: 389–400 (in Japanese).